emerald PUBLISHING

International Journal of Intelligent Unmanned Sy

Nonlinear optimal control for UAVs with tilting rotors

Journal:	*International Journal of Intelligent Unmanned Systems*
Manuscript ID	IJIUS-02-2023-0018
Manuscript Type:	Research Paper
Keywords:	tilt-rotor UAVs, differential flatness properties, nonlinear H-infinity control, Taylor series expansion, Jacobian matrices, Riccati equation

Nonlinear optimal control for UAVs with tilting rotors

G. Rigatos[a] M. Abbaszadeh[b] B. Sari[c] J. Pomares[d]

aUnit of Industrial Autom. ndustrial Systems Institute
bDept. of ECS Engineering Rensselaer Polytechnic Inst.
cDept. of Electrical Eng. University of Setif
dDept. of Systems Eng. University of Alicante

Abstract: A distinctive feature of tilt-rotor UAVs is that they can be fully actuated whereas in fixed-angle rotor UAVs (e.g. common-type quadrotors, octorotors etc.) the associated dynamic model is characterized by underactuation. Because of the existence of more control inputs, in tilt-rotor UAVs there is more flexibility in the solution of the associated nonlinear control problem. On the other side the dynamic model of the tilt-rotor UAVs remains nonlinear and multi-variable and this imposes difficulty in the drone's controller design. To achieve simultaneously precise tracking of trajectories and minimization of energy dissipation by the UAV's rotors elaborated control methods have to be developed. In the present article a solution of the nonlinear optimal control problem of tilt-rotor UAV's is attempted using a novel nonlinear optimal control method. This method is characterized by computational simplicity, clear implementation stages and proven global stability properties. At a first stage, approximate linearization is performed on the dynamic model of the tilt-rotor UAV with the use of first-order Taylor series expansion and through the computation of the system's Jacobian matrices. This linearization process is carried out at each sampling instance, around a temporary operating point which is defined by the present value of the tilt-rotor UAV's state vector and by the last sampled value of the control inputs vector. At a second stage, an H-infinity stabilizing controller is designed for the approximately linearized model of the tilt-rotor UAV. To find the feedback gains of the controller an algebraic Riccati equation is repetitively solved, at each time-step of the control method. Lyapunov stability analysis is used to prove the global stability properties of the control scheme. Moreover, the H-infinity Kalman Filter is used as a robust observer so as to enable state estimation-based control. The article's nonlinear optimal control approach achieves fast and accurate tracking of reference setpoints under moderate variations of the control inputs.

Keywords: tilt-rotor UAVs, differential flatness properties, nonlinear H-infinity control, Taylor series expansion, Jacobian matrices, Riccati equation, global stability.

1 Introduction

Aerial drones are widely used for civil and defence tasks and the solution of the associated nonlinear control, filtering and estimation problems is becoming a necessity [1-5]. Tilt-rotor UAVs are a specific type of aerial drones where the actuators (rotors) can move within a tilting angle around a reference axis [6 -10]. In fixed-angle rotor UAVs (e.g. common-type quadrotors, hexarotors, octorotors etc.) one has to modify the turn speed of the rotors so as to generate torques and thrust forces that will allow the drone's state variables converge to their setpoints and will make the drone follow the specified reference trajectories [11-15]. However, in tilt-rotor UAVs one can primarily modify the tilting angles of the rotors and can use these angles as control inputs so as to make the drone follow the designated paths and accomplish its flight plans [16-21]. Unlike fixed-angle rotor UAVs where the associated dynamic model is characterized by underactuation, tilt-rotor UAVs can be fully actuated [22-28]. The existence of more control inputs gives more flexibility in the solution of the UAV's nonlinear control problem [29-31]. The primary control objective remains to achieve simultaneously precise tracking of trajectories and minimization of energy dissipation by the UAV's rotors [32 -36]. In this context the implementation of nonlinear optimal control

in tilt-rotor UAVs remains a technical challenge.

So far nonlinear model predictive control (NMPC) methods have been of questionable performance in treating the nonlinear optimal control problem for tilt-rotor UAVs because NMPC's convergence to optimum depends often on the empirical selection of parameters while also lacking a global stability proof. In the present article a novel nonlinear optimal control method is proposed for solving the nonlinear optimal control problem of tilt-rotor UAV's. First, by following the assumption of small tilting angles the state-space model of the UAV is formulated and conditions of differential flatness are given about it [4]. Next, to implement the nonlinear optimal control method the dynamic model of the tilt-rotor UAV undergoes approximate linearization at each sampling instance around a temporary operating point which is defined by the present value of the system's state vector and by the last sampled value of the control inputs vector. The linearization process is based on first-order Taylor series expansion and on the computation of the associated Jacobian matrices [37-39]. The modelling error, which is due to the truncation of higher-order terms from the Taylor series, is considered to be a perturbation that is asymptotically compensated by the robustness of the control scheme.

For the linearized model of the UAV an H-infinity stabilizing feedback controller is designed. Actually, this H-infinity controller stands for the solution of the optimal control problem for the UAV under model uncertainty [1-3]. Furthermore , it represents a min-max differential game taking place between: (i) the control inputs which try to minimize a quadratic function of the state vector's tracking error, (ii) the modelling error and external perturbations which try to maximize this cost function. To select the feedback gains of the H-infinity controller an algebraic Riccati equation has to be repetitively solved at each time-step of the control method [40-41]. The stability properties of the control scheme are analyzed with the Lyapunov method. First, it is demonstrated that the H-infinity tracking performance holds, which signifies elevated robustness to model uncertainty and external disturbances [1-3]. [42]. Moreover, under moderate conditions, the global asymptotic stability properties of the control scheme are proven [1-3]. Finally, to implement state estimation-based control, the H-infinity Kalman Filter is used as a robust state estimator.

The proposed nonlinear optimal control method achieves fast and accurate tracking of setpoints by all state variables of the tilt-rotor UAV under moderate variations of the control inputs. The article has a meaningful contribution to the area of nonlinear control [1-4]. Comparing to past approaches for treating the nonlinear optimal (H-infinity) control problem, the article's approach is applicable also to dynamical systems which have a non-constant control inputs gain matrix. Furthermore, it uses a new Riccati equation to compute the controller's gains and follows a novel Lyapunov analysis to prove global stability for the control loop. It is also noteworthy that the nonlinear optimal control method is applicable to a wider class of dynamical systems than approaches based on the solution of State Dependent Riccati Equations (SDRE). The SDRE approaches can be applied only to dynamical systems which can be transformed to the Linear Parameter Varying (LPV) form. Besides, the nonlinear optimal control method performs better than nonlinear optimal control schemes which use approximation of the solution of the Hamilton-Jacobi-Bellman equation by Galerkin series expansions. The stability properties of the Galerkin series expansion -based optimal control approaches are still unproven.

The structure of the article is as follows: In Section 2 the dynamic model of the tilt-rotor UAV is formulated in state-space form and its differential flatness properties are analyzed. In Section 3 the dynamic model of the UAV undergies approximate linearization with the use of first-order Taylor series expansion and through the computation of the associated Jacobian matrices. Moreover a stabilizing H-infinity feedback controller is designed for this system. In Section 4 the global stability properties of the control scheme are proven through Lyapunov analysis. Besides, the H-infinity Kalman Filter is introduced as a robust state estimator. In Section 5 the tracking performance of the proposed control method is tested through simulation experiments. Finally in Section 6 concluding remarks are stated.

2 Dynamic model of the tilt-rotor UAV

2.1 The state-space model of the tilt-rotor UAV

The diagram of the tilt-rotor (quadrotor) UAV and the associated body-fixed and inertial reference frames are depicted in Fig. 1. Two reference frames are defined. The first one $B = [B_1, B_2, B_3]$ is attached to the quadropter's body, whereas the second $E = [E_x, E_y, E_z]$ is considered to be an inertial coordinates system. The Euler angles defining rotation round the axes of the inertial reference frame E_1, E_2 and E_3 are given as θ, ϕ and ψ, respectively. The two reference frames are connected to each other through a rotation matrix [1-4]

$$R = \begin{pmatrix} C\psi C\theta & C\psi S\theta S\phi - S\psi C\phi & C\psi S\theta C\phi + S\psi S\phi \\ S\psi C\theta & S\psi S\theta S\phi + C\psi C\phi & S\psi S\theta C\phi - C\psi S\phi \\ -S\theta & C\theta S\phi & C\theta C\phi \end{pmatrix} \tag{1}$$

where $C = cos(\cdot)$ and $S = sin(\cdot)$. The connection between velocities in the two reference frames is as follows:

$$V_E = R \cdot V_B \tag{2}$$

where $V_E = [u_E, v_E, w_E]$ and $V_B = [u_B, v_B, w_B]$ are the linear velocity vectors expressed in the two reference frames. About the angular velocities in the two reference frames the following relation holds

$$\dot{\eta} = W^{-1}\omega \tag{3}$$

that is

$$\begin{pmatrix} \dot{\phi} \\ \dot{\theta} \\ \dot{\psi} \end{pmatrix} = \begin{pmatrix} 1 & sin(\phi)tan(\theta) & cos(\phi)tan(\theta) \\ 0 & cos(\phi) & -sin(\phi) \\ 0 & sin(\phi)sec(\theta) & cos(\phi)sec(\theta) \end{pmatrix} \begin{pmatrix} p \\ q \\ r \end{pmatrix} \tag{4}$$

where $\eta = [\phi, \theta, \psi]^T$ is the angular velocities vector in the inertial reference frame and $\omega = [p, q, r]^T$ is the angular velocities vector in the body-fixed reference frame. The state vector of the tilt-rotor UAV in the inertial reference frame is $x = [x, y, z, \phi, \theta, \psi]^T$ and the associated velocities vector is $\dot{x} = [\dot{x}, \dot{y}, \dot{z}, \dot{\phi}, \dot{\theta}, \dot{\phi}]^T$. The tilting angles of the rotors are denoted as $\theta_i,\ i = 1, 2, 3, 4$.
The equations of linear motion of the UAV along the axes of the inertial reference frame are [29-31], [32 -36]

$$\begin{aligned} m\ddot{x} &= \sum F_i(sin(\phi)sin(\phi) + cos(\phi)sin(\theta)cos(\psi)) - C_1\dot{x} \\ m\ddot{y} &= \sum F_i(sin(\psi)sin(\theta)cos(\psi) - cos(\psi)sin(\phi)) - C_2\dot{\psi} \\ m\ddot{z} &= \sum F_i(cos(\theta)cos(\phi))) - mg - C_3\dot{z} \end{aligned} \tag{5}$$

where m is the mass of the drone. The thrust forces of the UAV's rotors are $F_i = K_f\omega_i^2$, with ω_i to be the turn speed of the i-th rotor and K_f to be a constant, while $C_i,\ i = 1, 2, 3$ are damping coefficients. About the rotational motion of the UAV, one has the following dynamics of the Euler angles $[\phi, \theta, \psi]$ of the drone [29-31], [32 -36]:

$$\begin{aligned} I_x\ddot{\phi} &= l(F_3 - F_1 - C_1^{'}\dot{\phi}) \\ I_y\ddot{\theta} &= l(F_4 - F_2 - C_2^{'}\dot{\theta}) \\ I_z\ddot{\psi} &= M_1 - M_2 + M_3 - M_4 - C_3^{'}\dot{\psi} \end{aligned} \tag{6}$$

where l is the distance of each rotor from the UAV's center of gravity, I_x, I_y, I_z are moments of inertia for rotational motion around the x, y and z axis, respectively. Moreover, $C_i^{'},\ i = 1, 2, 3$ are friction coefficients. M_i are the moments which are produced about the rotors of the UAV and about which holds

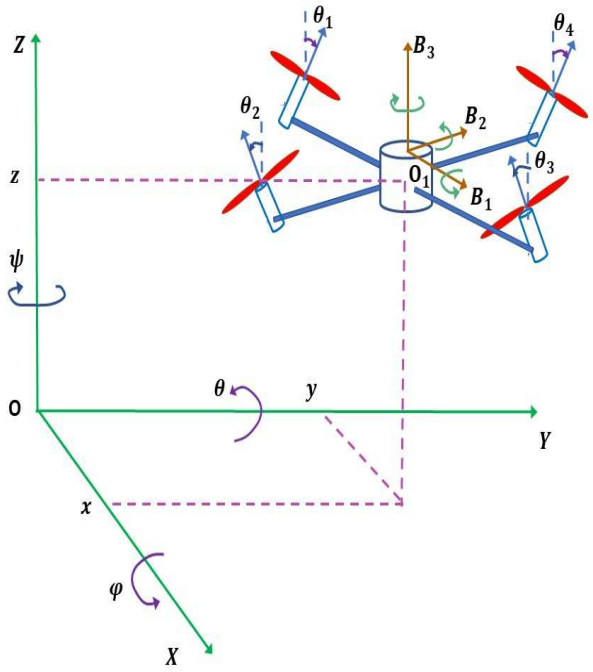

Figure 1: Diagram of the tilt-rotor (quadrotor) UAV and the associated body-fixed and inertial reference frames

$M_i = k_m\omega_i^2,\ i = 1, \cdots, 4$ with ω_i to be the turn speed of the i-th motor and k_i to be a constant.

The rotors of the UAV are allowed to tilt by angle $\theta_i,\ i = 1, \cdots, 4$ with reference to their transversal axis. The equations of linear motion of the tilt-rotor UAV with respect to the axes of the inertial reference frame are as follows: [29-31], [32 -36]

$$\begin{gathered} m\ddot{x} = F_1 sin(\theta_1)cos(\psi)cos(\theta) - F_3 sin(\theta_3)cos(\psi)cos(\theta) - F_4 sin(\theta_4)cos(\psi)sin(\theta)sin(\phi) \\ +F_4 sin(\theta_4)sin(\psi)cos(\phi) + F_2 sin(\theta_2)cos(\psi)sin(\theta)sin(\phi) - F_2 sin(\theta_2)sin(\psi)cos(\phi) \\ +F_1 cos(\theta_1)cos(\psi)sin(\theta)cos(\phi) + F_2 cos(\theta_2)cos(\psi)sin(\theta)cos(\phi) \\ +F_3 cos(\theta_3)cos(\psi)sin(\theta)cos(\phi) + F_4 cos(\theta_4)cos(\psi)sin(\theta)cos(\phi) + F_1 cos(\theta_1)sin(\psi)sin(\phi) \\ +F_2 cos(\theta_2)sin(\psi)sin(\phi) + F_3 cos(\theta_3)sin(\psi)sin(\phi) + F_4 cos(\theta_4)sin(\psi)sin(\phi) - C_1\dot{x} \end{gathered} \tag{7}$$

$$\begin{gathered} m\ddot{y} = F_1 sin(\theta_1)cos(\psi)cos(\theta) - F_3 sin(\theta_3)sin(\psi)cos(\theta) - F_4 sin(\theta_4)sin(\psi)sin(\theta)sin(\phi) + \\ +F_2 sin(\theta_2)sin(\psi)sin(\theta)sin(\phi) - F_4 sin(\theta_4)cos(\psi)cos(\phi) + F_2 sin(\theta_2)cos(\psi)cos(\phi) + \\ +F_1 cos(\theta_1)sin(\psi)sin(\theta)cos(\phi) + F_2 cos(\theta_2)sin(\psi)sin(\theta)cos(\phi) + \\ +F_3 cos(\theta_1)sin(\psi)sin(\theta)cos(\phi) + F_4 cos(\theta_4)sin(\psi)sin(\theta)cos(\phi) + F_1 cos(\theta_1)cos(\psi))sin(\phi) + \\ -F_2 cos(\theta_2)cos(\psi)sin(\phi) - F_3 cos(\theta_3)cos(\psi)cos(\phi) - F_4 cos(\theta_4)cos(\psi)cos(\phi) - C_2\dot{y} \end{gathered} \tag{8}$$

$$\begin{gathered} m\ddot{z} = -F_1 sin(\theta_1)sin(\theta) + F_3 sin(\theta_3)sin(\theta) - F_4 sin(\theta_4)cos(\theta)sin(\phi) + \\ +F_2 sin(\theta_2)cos(\theta)sin(\phi) + F_1 cos(\theta_1)cos(\theta)cos(\phi) + F_2 cos(\theta_2)cos(\theta)cos(\phi) + \\ +F_3 cos(\theta_3)cos(\theta)cos(\phi) + F_4 cos(\theta_4)cos(\theta)cos(\phi) - mgC_3\dot{z} \end{gathered} \tag{9}$$

Moreover, the equations of the rotational motion of the tilt-rotor UAV are given by [29-31], [32 -36]:

$$I_x\ddot{\phi} = l(F_3 cos(\theta_3) - F_1 cos(\theta_1) - C_1^{'}\dot{\phi}) + (M_1 sin(\theta_1) - M_3 sin(\theta_3)) + M_2^{'} + M_4^{'} \tag{10}$$

$$I_y\ddot{\theta} = l(F_4cos(\theta_4) - F_2cos(\theta_2) - C_2^{'}\dot{\theta}) + (M_4sin(\theta_4) - M_2sin(\theta_2)) + M_1^{'} + M_3^{'} \tag{11}$$

$$\begin{gathered} I_z\ddot{\psi} = l(F_1sin(\theta_1) + F_2sin(\theta_2) + F_3sin(\theta_3) + F_4sin(\theta_4) - C_3\dot{\psi}) + \\ +(M_1cos(\theta_1) - M_2cos(\theta_2) + M_3cos(\theta_3) - M_4cos(\theta_4)) \end{gathered} \tag{12}$$

Next, a small angle assumption is made about the tilting of the UAV's rotors, which signifies: $sin(\theta_1) \simeq \theta_1$, $cos(\theta_1) \simeq 1$, $sin(\theta_2) \simeq \theta_2$, $cos(\theta_2) \simeq 1$, $sin(\theta_3) \simeq \theta_3$, $cos(\theta_3) \simeq 1$ and $sin(\theta_4) \simeq \theta_4$, $cos(\theta_4) \simeq 1$. Thus, the dynamic model of the UAV becomes:

$$\begin{gathered} m\ddot{x} = F_1\theta_1cos(\psi)cos(\theta) - F_3\theta_3cos(\psi)cos(\theta) - F_4\theta_4cos(\psi)sin(\theta)sin(\phi) \\ +F_4\theta_4sin(\psi)cos(\phi) + F_2\theta_2cos(\psi)sin(\theta)sin(\phi) - F_2\theta_2sin(\psi)cos(\phi) \\ +F_1cos(\psi)sin(\theta)cos(\phi) + F_2cos(\psi)sin(\theta)cos(\phi) \\ +F_3cos(\psi)sin(\theta)cos(\phi) + F_4cos(\psi)sin(\theta)cos(\phi) + F_1sin(\psi)sin(\phi) \\ +F_2sin(\psi)sin(\phi) + F_3sin(\psi)sin(\phi) + F_4sin(\psi)sin(\phi) - C_1\dot{x} \end{gathered} \tag{13}$$

$$\begin{gathered} m\ddot{y} = F_1\theta_1cos(\psi)cos(\theta) - F_3\theta_3sin(\psi)cos(\theta) - F_4\theta_4sin(\psi)sin(\theta)sin(\phi) + \\ +F_2\theta_2sin(\psi)sin(\theta)sin(\phi) - F_4\theta_4cos(\psi)cos(\phi) + F_2\theta_2cos(\psi)cos(\phi) + \\ +F_1sin(\psi)sin(\theta)cos(\phi) + F_2sin(\psi)sin(\theta)cos(\phi) + \\ +F_3sin(\psi)sin(\theta)cos(\phi) + F_4sin(\psi)sin(\theta)cos(\phi) + F_1cos(\psi))sin(\phi) + \\ -F_2cos(\psi)sin(\phi) - F_3cos(\psi)cos(\phi) - F_4cos(\psi)cos(\phi) - C_2\dot{y} \end{gathered} \tag{14}$$

$$\begin{gathered} m\ddot{z} = -F_1\theta_1sin(\theta) + F_3\theta_3sin(\theta) - F_4\theta_4cos(\theta)sin(\phi) + \\ +F_2\theta_2cos(\theta)sin(\phi) + F_1cos(\theta)cos(\phi) + F_2cos(\theta)cos(\phi) + \\ +F_3cos(\theta)cos(\phi) + F_4cos(\theta)cos(\phi) - mgC_3\dot{z} \end{gathered} \tag{15}$$

$$I_x\ddot{\phi} = l(F_3 - F_1 - C_1^{'}\dot{\phi}) + (M_1\theta_1 - M_3\theta_3) + M_2^{'} + M_4^{'} \tag{16}$$

$$I_y\ddot{\theta} = l(F_4 - F_2 - C_2^{'}\dot{\theta}) + (M_4\theta_4 - M_2\theta_2) + M_1^{'} + M_3^{'} \tag{17}$$

$$\begin{gathered} I_z\ddot{\psi} = l(F_1\theta_1 + F_2\theta_2 + F_3\theta_3 + F_4\theta_4 - C_3\dot{\psi}) + \\ +(M_1 - M_2 + M_3 - M_4) \end{gathered} \tag{18}$$

In the above equations of the rotational dynamics of the tilt-rotor UAV, parameters $M_i^{'}$ denote the tilting angle torques of the UAV's motors. Next, it is considered that the UAV avoids aggressive maneuvers and thus the roll and pitch angles of the UAV remain at small values. Thus, it holds $sin(\phi) \simeq \phi$, $cos(\phi) \simeq 1$ and $sin(\theta) \simeq \theta$, $cos(\theta) \simeq 1$. On the other side, it is considered that the yaw angle ψ of the UAV may vary without constraints, that is the drone can turn around the z axis so as to change its heading. Thus the dynamics of the tilt-rotor UAV becomes:

$$\begin{gathered} m\ddot{x} = F_1\theta_1cos(\psi) - F_3\theta_3cos(\psi) - F_4\theta_4cos(\psi)\theta\phi \\ +F_4\theta_4sin(\psi) + F_2\theta_2cos(\psi)\theta\phi - F_2\theta_2sin(\psi) \\ +F_1cos(\psi)\theta + F_2cos(\psi)\theta \\ +F_3cos(\psi)\theta + F_4cos(\psi)\theta + F_1sin(\psi)\phi \\ +F_2sin(\psi)\phi + F_3sin(\psi)\phi + F_4sin(\psi)\phi - C_1\dot{x} \end{gathered} \tag{19}$$

$$\begin{gathered} m\ddot{y} = F_1\theta_1cos(\psi) - F_3\theta_3sin(\psi) - F_4\theta_4sin(\psi)\theta\phi + \\ +F_2\theta_2sin(\psi)\theta\phi - F_4\theta_4cos(\psi) + F_2\theta_2cos(\psi) + \\ +F_1sin(\psi)\theta + F_2sin(\psi)\theta + \\ +F_3sin(\psi)\theta + F_4sin(\psi)\theta + F_1cos(\psi))\phi + \\ -F_2cos(\psi)\phi - F_3cos(\psi) - F_4cos(\psi) - C_2\dot{y} \end{gathered} \tag{20}$$

$$m\ddot{z} = -F_1\theta_1\theta + F_3\theta_3\theta - F_4\theta_4\phi + \\ +F_2\theta_2\phi + F_1 + F_2 + \\ +F_3 + F_4 - mgC_3\dot{z} \tag{21}$$

$$I_x\ddot{\phi} = l(F_3 - F_1 - C_1^{'}\dot{\phi}) + (M_1\theta_1 - M_3\theta_3) + M_2^{'} + M_4^{'} \tag{22}$$

$$I_y\ddot{\theta} = l(F_4 - F_2 - C_2^{'}\dot{\theta}) + (M_4\theta_4 - M_2\theta_2) + M_1^{'} + M_3^{'} \tag{23}$$

$$I_z\ddot{\psi} = l(F_1\theta_1 + F_2\theta_2 + F_3\theta_3 + F_4\theta_4 - C_3\dot{\psi}) + \\ +(M_1 - M_2 + M_3 - M_4) \tag{24}$$

Next, by denoting the state-vector of the tilt-rotor UAV as

$$x = [x_1x_2, x_3, x_4, x_5, x_6, x_7, x_8, x_9, x_{10}, x_{11}, x_{12}]^T \Rightarrow \\ x = [x, \dot{x}, y, \dot{y}, z, \dot{z}, \phi, \dot{\phi}, \theta, \dot{\theta}, \psi, \dot{\psi}]^T \tag{25}$$

Moreover, the control inputs vector of the tilt-rotor UAV is extended by considering as additional control inputs the torques $\bar{\tau}_1 = l(F_3 - F_1)$ in Eq. (22) and $\bar{\tau}_2 = l(F_4 - F_2)$ in Eq. (23). Thus, the control inputs vector of the tilt-rotor UAV becomes $u = [u_1, u_2, u_3, u_4, u_5, u_6]^T$ or $u = [\theta_1, \theta_2, \theta_3, \theta_4, \bar{\tau}_1, \bar{\tau}_2]^T$.

$$u = [u_1, u_2, u_3, u_4, u_5, u_6]^T \Rightarrow u = [\theta_1, \theta_2, \theta_3, \theta_4, \bar{\tau}_1, \bar{\tau}_2]^T \tag{26}$$

the dynamic model of the tilt-rotor UAV is written as

$$\dot{x}_1 = x_2 \tag{27}$$

$$\dot{x}_2 = \tfrac{1}{m}\{F_1\theta_1 cos(x_{11}) - F_3\theta_3 cos(x_{11}) - F_4\theta_4 cos(x_{11})x_7x_9 \\ +F_4\theta_4 sin(x_{11}) + F_2\theta_2 cos(x_{11})x_7x_9 - F_2\theta_2 sin(x_{11}) \\ +F_1 cos(x_{11})x_9 + F_2 cos(x_{11})x_9 \\ +F_3 cos(x_{11})x_9 + F_4 cos(x_{11})x_9 + F_1 sin(x_{11})x_7 \\ +F_2 sin(x_{11})x_7 + F_3 sin(x_{11})x_7 + F_4 sin(x_{11})x_7 - C_1x_2\} \tag{28}$$

$$\dot{x}_3 = x_4 \tag{29}$$

$$\dot{x}_4 = \tfrac{1}{m}\{F_1\theta_1 cos(x_{11}) - F_3\theta_3 sin(x_{11}) - F_4\theta_4 sin(x_{11})x_7x_9 + \\ +F_2\theta_2 sin(x_{11})x_7x_9 - F_4\theta_4 cos(x_{11}) + F_2\theta_2 cos(x_{11}) + \\ +F_1 sin(x_{11})x_9 + F_2 sin(x_{11})x_9 + \\ +F_3 sin(x_{11})x_9 + F_4 sin(x_{11})x_9 + F_1 cos(x_{11}))x_7 + \\ -F_2 cos(x_{11})x_7 - F_3 cos(x_{11}) - F_4 cos(x_{11}) - C_2x_4\} \tag{30}$$

$$\dot{x}_5 = x_6 \tag{31}$$

$$\ddot{x}_6 = \tfrac{1}{m}\{-F_1\theta_1x_9 + F_3\theta_3x_9 - F_4\theta_4x_7 + \\ +F_2\theta_2x_7 + F_1 + F_2 + \\ +F_3 + F_4 - mgC_3x_6\} \tag{32}$$

$$\dot{x}_7 = x_8 \tag{33}$$

$$\dot{x}_8 = \tfrac{1}{I_x}\{l(-C_1^{'}x_8) + (M_1\theta_1 - M_3\theta_3) + (M_2^{'} + M_4^{'})\} + \tfrac{1}{I_x}\bar{\tau}_1 \tag{34}$$

$$\dot{x}_9 = x_{10} \tag{35}$$

$$\dot{x}_{10} = \frac{1}{I_y}\{l(-C_2^{'}x_{10}) + (M_4\theta_4 - M_2\theta_2) + (M_1^{'} + M_3{'})\} + \frac{1}{I_y}\bar{\tau}_2 \tag{36}$$

$$\dot{x}_{11} = x_{12} \tag{37}$$

$$\dot{x}_{12} = \frac{1}{I_z}\{l(F_1\theta_1 + F_2\theta_2 + F_3\theta_3 + F_4\theta_4 - C_3\dot{\psi}) + \\ +(M_1 - M_2 + M_3 - M_4)\} \tag{38}$$

Consequently, the state-space model of the tilt-rotor UAV is written in the following state-space form

$$\begin{pmatrix} \dot{x}_1 \\ \dot{x}_2 \\ \dot{x}_3 \\ \dot{x}_4 \\ \dot{x}_5 \\ \dot{x}_6 \\ \dot{x}_7 \\ \dot{x}_8 \\ \dot{x}_9 \\ \dot{x}_{10} \\ \dot{x}_{11} \\ \dot{x}_{12} \end{pmatrix} = \begin{pmatrix} x_2 \\ \frac{1}{m}\{(F_1+F_2+F_3+F_4)cos(x_{11}x_9 + (F_1+F_2+F_3+F_4)sin(x_{11}x_7 - C_1x_2\} \\ x_4 \\ \frac{1}{m}\{(F_1+F_2+F_3+F_4)sin(x_{11}x_9 - (F_1+F_2+F_3+F_4)cos(x_{11}x_7 - C_2x_4\} \\ x_6 \\ \frac{1}{m}\{(F_1+F_2+F_3+F_4) - mg - C_3x_6\} \\ x_8 \\ \frac{1}{I_x}\{l(-C_1^{'}x_8)) + (M_2^{'} + M_4^{'})\} \\ x_{10} \\ \frac{1}{I_y}\{l(-C_2^{'}x_{10})) + (M_1^{'} + M_3^{'})\} \\ x_{12} \\ \frac{1}{I_z}\{-lC_3^{'}x_{12}) + (M_1 - M_2 + M_3 - M_4)\} \end{pmatrix} +$$

$$\begin{pmatrix} 0 & 0 & 0 & 0 & 0 & 0 \\ \frac{1}{m}F_1cos(x_{11}) & \frac{1}{m}[-F_2sin(x_{11}+F_2cos(x_{11}x_7x_9))] & \frac{1}{m}F_3cos(x_{11}) & \frac{1}{m}[F_4sin(x_{11}+F_4cos(x_{11}x_7x_9))] & 0 & 0 \\ 0 & 0 & 0 & 0 & 0 & 0 \\ \frac{1}{m}F_1cos(x_{11}) & \frac{1}{m}[F_2+F_2sin(x_{11}x_7x_9))] & -\frac{1}{m}F_3sin(x_{11}) & \frac{1}{m}[-F_4-F_4sin(x_{11}x_7x_9))] & 0 & 0 \\ 0 & 0 & 0 & 0 & 0 & 0 \\ -\frac{1}{m}F_1x_9 & \frac{1}{m}F_2x_7 & \frac{1}{m}F_3x_9 & -\frac{1}{m}F_4x_7 & 0 & 0 \\ 0 & 0 & 0 & 0 & 0 & 0 \\ \frac{M_1}{I_x} & 0 & -\frac{M_3}{I_x} & 0 & \frac{1}{I_x} & 0 \\ 0 & 0 & 0 & 0 & 0 & 0 \\ 0 & -\frac{M_2}{I_y} & 0 & \frac{M_4}{I_y} & 0 & \frac{1}{1_y} \\ 0 & 0 & 0 & 0 & 0 & 0 \\ \frac{lF_1}{I_z} & \frac{lF_2}{I_z} & \frac{lF_3}{I_z} & \frac{lF_4}{I_z} & 0 & 0 \end{pmatrix} \begin{pmatrix} u_1 \\ u_2 \\ u_3 \\ u_4 \\ u_5 \\ u_6 \end{pmatrix} \tag{39}$$

Consequently, the dynamic model of the tilt-rotor UAV can be written in the nonlinear affine-in-the-input state-space form:

$$\dot{x} = f(x) + g(x)u \tag{40}$$

where $x \in R^{12\times1}$, $f(x) \in R^{12\times1}$, $g(x) \in R^{12\times6}$, and $u \in R^{6\times1}$.

2.2 Differential flatness properties of the dynamic model of the tilt-rotor UAV

As explained above, if one considers as control inputs only the tilt angles of the rotors, the tilt-rotor UAV is an underactuated system that has 6-DOF and 4 control inputs. By using also the torque variables $\bar{\tau}_1 = l(F_3 - F1)$ and $\bar{\tau}_2 = l(F_4 - F_2)$ as additional control inputs the system becomes fully actuated.

For the case of full actuation, the tilt-rotor UAV is also a differentially flat system with flat output vector $Y = [x_1.x_3, x_5, x_7.x_9, x_{11}]^T$. Indeed it holds that

$$\begin{array}{lll} x_2 = \dot{x}_1 & x_4 = \dot{x}_3 & x_6 = \dot{x}_5 \\ x_8 = \dot{x}_7 & x_{10} = \dot{x}_9 & x_{12} = \dot{x}_{11} \end{array} \tag{41}$$

which signifies that state variables x_2, x_4, x_6, x_8, x_{10} and x_{12} are differential functions of the flat outputs of the system. Besides from the even-numbered rows of the state-space model of the tilt-rotor UAV one has

$$\begin{array}{ll} \dot{x}_2 = \tilde{f}_2(x, u_1, u_2, u_3, u_4, u_5, u_6) & \dot{x}_4 = \tilde{f}_4(x, u_1, u_2, u_3, u_4, u_5, u_6) \\ \dot{x}_6 = \tilde{f}_6(x, u_1, u_2, u_3, u_4, u_5, u_6) & \dot{x}_8 = \tilde{f}_8(x, u_1, u_2, u_3, u_4, u_5, u_6) \\ \dot{x}_{10} = \tilde{f}_{10}(x, u_1, u_2, u_3, u_4, u_5, u_6) & \dot{x}_{12} = \tilde{f}_{12}(x, u_1, u_2, u_3, u_4, u_5, u_6) \end{array} \tag{42}$$

Thus one has a system of 6 equations which can be solved for u_1, u_2, u_3, u_4, u_5, u_6. Consequently, the control inputs can be also written as differential functions of the flat outputs and the tilt-rotor UAV is proven to be a differentially flat system [2].

3 Linearization and design of a stabilizing H-infinity feedback controller

3.1 Approximate linearization of the dynamic model of the tilt-rotor UAV

The dynamic model of the tilt-rotor UAV undergoes approximate linearization around the temporary operating point (x^*, u^*) at each sampling instance, where x^* is the present value of the system's state vector and u^* is the last sampled value of the control inputs vector. The linearization is based on 1-st order Taylor series expansion and on the computation of the associated Jacobian matrices. The modelling error which is due to the truncation of higher-order terms from the Taylor series is considered to be a perturbation that is asymptotically compensated by the robustness of the control algorithm. The linearization process gives:

$$\dot{x} = Ax + Bu + \tilde{d} \tag{43}$$

where $\tilde{d}$ is the cumulative disturbance term which comprises: (a) modelling error due to the truncation of higher-order terms from the Taylor series expansion, (ii) exogenous perturbations, (iii) measurement noise of any distribution. It holds that A and B are the Jacobian matrices of the system which are computed as follows:

$$\begin{array}{c} A = \nabla_x [f(x) + g(x)] \mid_{(x^*, u^*)} \Rightarrow \\ A = \nabla_x f(x) \mid_{(x^*, u^*)} + \nabla_x g_1(x) u_1 \mid_{(x^*, u^*)} + \nabla_x g_2(x) u_2 \mid_{(x^*, u^*)} + \\ + \nabla_x g_3(x) u_3 \mid_{(x^*, u^*)} + \nabla_x g_4(x) u_4 \mid_{(x^*, u^*)} + \nabla_x g_5(x) u_5 \mid_{(x^*, u^*)} + \nabla_x g_6(x) u_6 \mid_{(x^*, u^*)} \end{array} \tag{44}$$

$$B = \nabla_u [f(x) + g(x)] \mid_{(x^*, u^*)} \Rightarrow B = g(x) \mid_{(x^*, u^*)} \tag{45}$$

This linearization approach which has been followed for implementing the nonlinear optimal control scheme results into a quite accurate model of the system's dynamics. Consider for instance the following affine-in-the-input state-space model

$$\begin{array}{c} \dot{x} = f(x) + g(x)u \Rightarrow \\ \dot{x} = [f(x^*) + \nabla_x f(x) \mid_{x^*} (x - x^*)] + [g(x^*) + \nabla_x g(x) \mid_{x^*} (x - x^*)]u^* + \\ + g(x^*)u^* + g(x^*)(u - u^*) + \tilde{d}_1 \Rightarrow \\ \dot{x} = [\nabla_x f(x) \mid_{x^*} + \nabla_x g(x) \mid_{x^*} u^*]x + g(x^*)u - [\nabla_x f(x) \mid_{x^*} + \\ + \nabla_x g(x) \mid_{x^*} u^*]x^* + f(x^*) + g(x^*)u^* + \tilde{d}_1 \end{array} \tag{46}$$

where $\tilde{d}_1$ is the modelling error due to truncation of higher order terms in the Taylor series expansion of $f(x)$ and $g(x)$. Next, by defining $A = [\nabla_x f(x) \mid_{x^*} + \nabla_x g(x) \mid_{x^*} u^*]$, $B = g(x^*)$ one obtains

$$\dot{x} = Ax + Bu - Ax^* + f(x^*) + g(x^*)u^* + \tilde{d}_1 \tag{47}$$

Moreover by denoting $\tilde{d} = -Ax^* + f(x^*) + g(x^*)u^* + \tilde{d}_1$ about the cumulative modelling error term in the Taylor series expansion procedure one has

$$\dot{x} = Ax + Bu + \tilde{d} \tag{48}$$

which is the approximately linearized model of the dynamics of the system of Eq. (43). The term $f(x^*) + g(x^*)u^*$ is the derivative of the state vector at (x^*, u^*) which is almost annihilated by $-Ax^*$.

The Jacobian matrix $\nabla_x f(x) \mid_{(x^*,u^*)}$ is computed as follows:

Computation of the Jacobian matrix $\nabla_x f(x) \mid_{x^*,u^*}$: The notation $\sum F = F_1 + F_2 + F_3 + F_4$ is used

$\nabla_x f(x) \mid_{(x^*,u^*)} =$

$$\begin{pmatrix}
0 & 1 & 0 & 0 & 0 & 0 & 0 & 0 & 0 & 0 & 0 & 0 \\
0 & \frac{-C_1}{m} & 0 & 0 & 0 & 0 & \frac{-\sum F}{m} sin(x_{11}) & 0 & \frac{\sum F}{m} cos(x_{11}) & 0 & \frac{\sum F}{m} q_1 & 0 \\
0 & 0 & 0 & 1 & 0 & 0 & 0 & 0 & 0 & 0 & 0 & 0 \\
0 & 0 & 0 & \frac{-C_2}{m} & 0 & 0 & \frac{-\sum F}{m} cos(x_{11}) & 0 & \frac{\sum F}{m} sin(x_{11}) & 0 & \frac{\sum F}{m} q_2 & 0 \\
0 & 0 & 0 & 0 & 0 & 1 & 0 & 0 & 0 & 0 & 0 & 0 \\
0 & 0 & 0 & 0 & 0 & \frac{-C_3}{m} & 0 & 0 & 0 & 0 & 0 & 0 \\
0 & 0 & 0 & 0 & 0 & 0 & 0 & 1 & 0 & 0 & 0 & 0 \\
0 & 0 & 0 & 0 & 0 & 0 & 0 & \frac{-C_1'}{I_x} & 0 & 0 & 0 & 0 \\
0 & 0 & 0 & 0 & 0 & 0 & 0 & 0 & 0 & 1 & 0 & 0 \\
0 & 0 & 0 & 0 & 0 & 0 & 0 & 0 & 0 & \frac{-C_2'}{I_y} & 0 & 0 \\
0 & 0 & 0 & 0 & 0 & 0 & 0 & 0 & 0 & 0 & 0 & 1 \\
0 & 0 & 0 & 0 & 0 & 0 & 0 & 0 & 0 & 0 & 0 & \frac{-C_3'}{I_z}
\end{pmatrix} \tag{49}$$

where $q_1 = [sin(x_{11})x_7 + cos(x_{11})x_8]$ and $q_2 = [-cos(x_{11})x_7 + sin(x_{11})x_9]$.

Computation of the Jacobian matrix $\nabla_x g_1(x) \mid_{x^*,u^*}$:

$$\nabla_x g_1(x) \mid_{(x^*,u^*)}=$$

$$\begin{pmatrix}
0 & 0 & 0 & 0 & 0 & 0 & 0 & 0 & 0 & 0 & 0 & 0 \\
0 & 0 & 0 & 0 & 0 & 0 & 0 & 0 & 0 & 0 & -\frac{1}{m}F_1 sin(x_{11}) & 0 \\
0 & 0 & 0 & 0 & 0 & 0 & 0 & 0 & 0 & 0 & 0 & 0 \\
0 & 0 & 0 & 0 & 0 & 0 & 0 & 0 & 0 & 0 & -\frac{1}{m}F_1 sin(x_{11}) & 0 \\
0 & 0 & 0 & 0 & 0 & 0 & 0 & 0 & 0 & 0 & 0 & 0 \\
0 & 0 & 0 & 0 & 0 & 0 & 0 & 0 & -\frac{F_1}{m} & 0 & 0 & 0 \\
0 & 0 & 0 & 0 & 0 & 0 & 0 & 0 & 0 & 0 & 0 & 0 \\
0 & 0 & 0 & 0 & 0 & 0 & 0 & 0 & 0 & 0 & 0 & 0 \\
0 & 0 & 0 & 0 & 0 & 0 & 0 & 0 & 0 & 0 & 0 & 0 \\
0 & 0 & 0 & 0 & 0 & 0 & 0 & 0 & 0 & 0 & 0 & 0 \\
0 & 0 & 0 & 0 & 0 & 0 & 0 & 0 & 0 & 0 & 0 & 0 \\
0 & 0 & 0 & 0 & 0 & 0 & 0 & 0 & 0 & 0 & 0 & 0
\end{pmatrix} \quad (50)$$

Computation of the Jacobian matrix $\nabla_x g_2(x)\mid_{x^*,u^*}$:

$$\nabla_x g_2(x)\mid_{(x^*,u^*)}=$$

$$\begin{pmatrix}
0 & 0 & 0 & 0 & 0 & 0 & 0 & 0 & 0 & 0 & 0 & 0\\
0 & 0 & 0 & 0 & 0 & 0 & \frac{1}{m}[F_2 cos(x_{11}x_9)] & 0 & \frac{1}{m}[F_2 cos(x_{11}x_7)] & 0 & -\frac{F_2}{m}cos(x_{11}) - sin(x_{11}x_7x_9) & 0\\
0 & 0 & 0 & 0 & 0 & 0 & 0 & 0 & 0 & 0 & 0 & 0\\
0 & 0 & 0 & 0 & 0 & 0 & \frac{1}{m}[F_2 sin(x_{11}x_9)] & 0 & \frac{1}{m}[F_2 sin(x_{11}x_7)] & 0 & \frac{F_2}{m}cos(x_{11}x_7x_9) & 0\\
0 & 0 & 0 & 0 & 0 & 0 & 0 & 0 & 0 & 0 & 0 & 0\\
0 & 0 & 0 & 0 & 0 & 0 & \frac{F_2}{m} & 0 & 0 & 0 & 0 & 0\\
0 & 0 & 0 & 0 & 0 & 0 & 0 & 0 & 0 & 0 & 0 & 0\\
0 & 0 & 0 & 0 & 0 & 0 & 0 & 0 & 0 & 0 & 0 & 0\\
0 & 0 & 0 & 0 & 0 & 0 & 0 & 0 & 0 & 0 & 0 & 0\\
0 & 0 & 0 & 0 & 0 & 0 & 0 & 0 & 0 & 0 & 0 & 0\\
0 & 0 & 0 & 0 & 0 & 0 & 0 & 0 & 0 & 0 & 0 & 0
\end{pmatrix} \tag{51}$$

Computation of the Jacobian matrix $\nabla_x g_3(x)\mid_{x^*,u^*}$:

$$\nabla_x g_3(x)\mid_{(x^*,u^*)}=$$

$$\begin{pmatrix}
0 & 0 & 0 & 0 & 0 & 0 & 0 & 0 & 0 & 0 & 0 & 0\\
0 & 0 & 0 & 0 & 0 & 0 & 0 & 0 & 0 & 0 & -\frac{1}{m}F_3 sin(x_{11}) & 0\\
0 & 0 & 0 & 0 & 0 & 0 & 0 & 0 & 0 & 0 & 0 & 0\\
0 & 0 & 0 & 0 & 0 & 0 & 0 & 0 & 0 & 0 & -\frac{1}{m}F_3 sin(x_{11}) & 0\\
0 & 0 & 0 & 0 & 0 & 0 & 0 & 0 & 0 & 0 & 0 & 0\\
0 & 0 & 0 & 0 & 0 & 0 & 0 & 0 & \frac{F_3}{m} & 0 & 0 & 0\\
0 & 0 & 0 & 0 & 0 & 0 & 0 & 0 & 0 & 0 & 0 & 0\\
0 & 0 & 0 & 0 & 0 & 0 & 0 & 0 & 0 & 0 & 0 & 0\\
0 & 0 & 0 & 0 & 0 & 0 & 0 & 0 & 0 & 0 & 0 & 0\\
0 & 0 & 0 & 0 & 0 & 0 & 0 & 0 & 0 & 0 & 0 & 0\\
0 & 0 & 0 & 0 & 0 & 0 & 0 & 0 & 0 & 0 & 0 & 0
\end{pmatrix} \tag{52}$$

Computation of the Jacobian matrix $\nabla_x g_4(x)\mid_{x^*,u^*}$:

$\nabla_x g_4(x) \mid_{(x^*,u^*)}=$

$$\begin{pmatrix}
0 & 0 & 0 & 0 & 0 & 0 & 0 & 0 & 0 & 0 & 0 & 0 \\
0 & 0 & 0 & 0 & 0 & 0 & \frac{1}{m}[F_4 cos(x_{11}x_9)] & 0 & \frac{1}{m}[F_4 cos(x_{11}x_7)] & 0 & \frac{F_4}{m}cos(x_{11}) - sin(x_{11}x_7x_9) & 0 \\
0 & 0 & 0 & 0 & 0 & 0 & 0 & 0 & 0 & 0 & 0 & 0 \\
0 & 0 & 0 & 0 & 0 & 0 & -\frac{1}{m}[F_4 sin(x_{11}x_9)] & 0 & -\frac{1}{m}[F_4 sin(x_{11}x_7)] & 0 & \frac{F_4}{m} - cos(x_{11}x_7x_9) & 0 \\
0 & 0 & 0 & 0 & 0 & 0 & 0 & 0 & 0 & 0 & 0 & 0 \\
0 & 0 & 0 & 0 & 0 & 0 & -\frac{F_4}{m} & 0 & 0 & 0 & 0 & 0 \\
0 & 0 & 0 & 0 & 0 & 0 & 0 & 0 & 0 & 0 & 0 & 0 \\
0 & 0 & 0 & 0 & 0 & 0 & 0 & 0 & 0 & 0 & 0 & 0 \\
0 & 0 & 0 & 0 & 0 & 0 & 0 & 0 & 0 & 0 & 0 & 0 \\
0 & 0 & 0 & 0 & 0 & 0 & 0 & 0 & 0 & 0 & 0 & 0 \\
0 & 0 & 0 & 0 & 0 & 0 & 0 & 0 & 0 & 0 & 0 & 0 \\
0 & 0 & 0 & 0 & 0 & 0 & 0 & 0 & 0 & 0 & 0 & 0
\end{pmatrix} \tag{53}$$

Moreover, it holds that $\nabla_x g_5(x) \mid_{(x^*,u^*)}= O_{12\times 12}$ and $\nabla_x g_6(x) \mid_{(x^*,u^*)}= O_{12\times 12}$. Thus the Jacobian matrices of the last two columns of the control inputs gain matrix $g(x)$ of the tilt-rotor UAV are zero matrices.

3.2 Stabilizing feedback control

After linearization around its current operating point (x^*, u^*), the dynamic model of the tilt-rotor UAV is written as [1]

$$\dot{x} = Ax + Bu + d_1 \tag{54}$$

Parameter d_1 stands for the linearization error in the tilt-rotor UAV 's model appearing previously in Eq. (54). The reference setpoints for the tilt-rotor UAV 's state vector are denoted by $\mathbf{x_d} = [x_1^d, \cdots, x_{12}^d]$. Tracking of this trajectory is achieved after applying the control input u^*. At every time instant the control input u^* is assumed to differ from the control input u appearing in Eq. (54) by an amount equal to Δu, that is $u^* = u + \Delta u$

$$\dot{x}_d = Ax_d + Bu^* + d_2 \tag{55}$$

The dynamics of the controlled system described in Eq. (54) can be also written as

$$\dot{x} = Ax + Bu + Bu^* - Bu^* + d_1 \tag{56}$$

and by denoting $d_3 = -Bu^* + d_1$ as an aggregate disturbance term one obtains

$$\dot{x} = Ax + Bu + Bu^* + d_3 \tag{57}$$

By subtracting Eq. (55) from Eq. (57) one has

$$\dot{x} - \dot{x}_d = A(x - x_d) + Bu + d_3 - d_2 \tag{58}$$

By denoting the tracking error as $e = x - x_d$ and the aggregate disturbance term as $\tilde{d} = d_3 - d_2$, the tracking error dynamics becomes

$$\dot{e} = Ae + Bu + \tilde{d} \tag{59}$$

For the approximately linearized model of the system a stabilizing feedback controller is developed. The controller has the form

$$u(t) = -Ke(t) \tag{60}$$

with $K = \frac{1}{r}B^T P$ where P is a positive definite symmetric matrix which is obtained from the solution of the Riccati equation [1]

$$A^T P + PA + Q - P(\tfrac{2}{r}BB^T - \tfrac{1}{\rho^2}LL^T)P = 0 \tag{61}$$

where Q is a positive semi-definite symmetric matrix. The previously analyzed concept about the nonlinear optimal control loop for the tilt-rotor's UAV is given in Fig. 2.

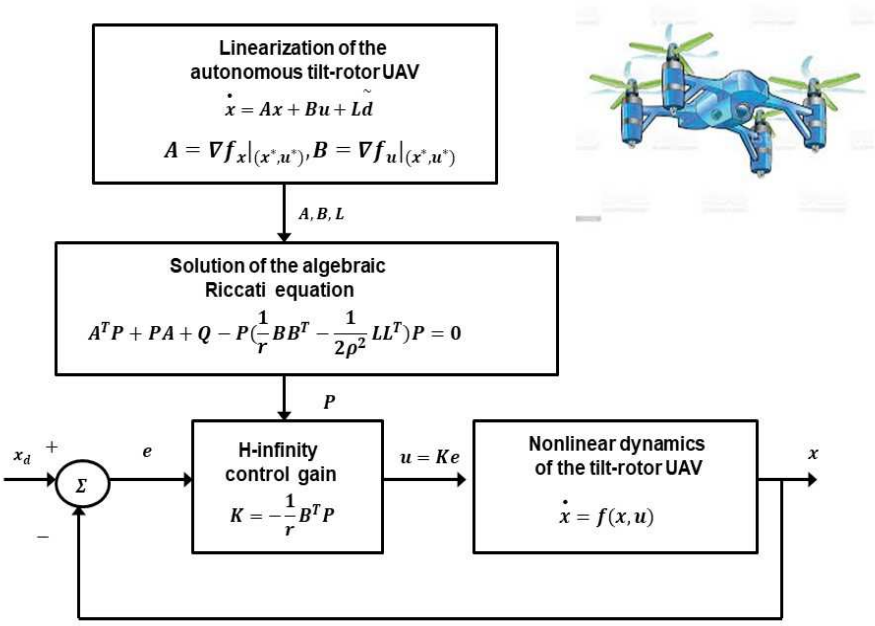

Figure 2: Diagram of the control scheme for the autonomous tilt-rotor (quadrotor) UAV

Whereas the Linear Quadratic Regulator (LQR) is the solution of the quadratic optimal control problem using Bellman's optimality principle, H-infinity control is the solution of the optimal control problem under model uncertainty and external perturbations. The cost function that is subject to minimization in the case of LQR comprises a quadratic term of the state vector's tracking error, as well as a quadratic term of the variations of the control inputs. In the case of H-infinity control the cost function is extended with the inclusion of a quadratic term of the cumulative disturbance and model uncertainty inputs that affect the model of the controlled system. In the case of the tilt-rotor UAV, the UAV's dynamic model is nonlinear and is also affected by uncertainty and external perturbations. By applying approximate linearization to the tilt-rotor UAV's dynamics one obtains a linear state-space description which is subject to modelling imprecision and exogenous disturbances. Therefore, one can arrive at a solution of the related optimal control problem only by applying the H-infinity control approach.

It is also noted that the solution of the H-infinity feedback control problem for the tilt-rotor UAV and the computation of the worst case disturbance that this controller can sustain, comes from superposition of Bellman's optimality principle when considering that the UAV is affected by two separate inputs (i) the control input u (ii) the cumulative disturbance input $\tilde{d}(t)$. Solving the optimal control problem for u that is for the minimum variation (optimal) control input that achieves elimination of the state vector's tracking error gives $u = -\frac{1}{r}B^T Pe$. Equivalently, solving the optimal control problem for $\tilde{d}$, that is for the worst case disturbance that the control loop can sustain gives $\tilde{d} = \frac{1}{\rho^2}L^T Pe$.

4 Lyapunov stability analysis

4.1 Global stability proof

Through Lyapunov stability analysis it will be shown that the proposed nonlinear control scheme assures H_∞ tracking performance for the autonomous tilt-rotor UAV, and that in case of bounded disturbance terms asymptotic convergence to the reference setpoints is achieved. The tracking error dynamics for the autonomous tilt-rotor UAV is written in the form

$$\dot{e} = Ae + Bu + L\tilde{d} \tag{62}$$

where in the tilt-rotor UAV's case $L = I \in R^{12\times 12}$ with I being the identity matrix. Variable $\tilde{d}$ denotes model uncertainties and external disturbances of the autonomous tilt-rotor UAV's model. The following Lyapunov equation is considered

$$V = \frac{1}{2}e^T Pe \tag{63}$$

where $e = x - x_d$ is the tracking error. By differentiating with respect to time one obtains

$$\begin{gathered}\dot{V} = \frac{1}{2}\dot{e}^T Pe + \frac{1}{2}e^T P\dot{e} \Rightarrow \\ \dot{V} = \frac{1}{2}[Ae + Bu + L\tilde{d}]^T Pe + \frac{1}{2}e^T P[Ae + Bu + L\tilde{d}] \Rightarrow \\ \dot{V} = \frac{1}{2}[e^T A^T + u^T B^T + \tilde{d}^T L^T]Pe + \frac{1}{2}e^T P[Ae + Bu + L\tilde{d}] \Rightarrow \\ \dot{V} = \frac{1}{2}e^T A^T Pe + \frac{1}{2}u^T B^T Pe + \frac{1}{2}\tilde{d}^T L^T Pe + \frac{1}{2}e^T PAe + \frac{1}{2}e^T PBu + \frac{1}{2}e^T PL\tilde{d}\end{gathered} \tag{64}$$

The previous equation is rewritten as

$$\dot{V} = \frac{1}{2}e^T(A^T P + PA)e + (\frac{1}{2}u^T B^T Pe + \frac{1}{2}e^T PBu) + (\frac{1}{2}\tilde{d}^T L^T Pe + \frac{1}{2}e^T PL\tilde{d}) \tag{65}$$

Assumption: For given positive definite matrix Q and coefficients r and ρ there exists a positive definite matrix P, which is the solution of the following matrix equation

$$A^T P + PA = -Q + P(\frac{2}{r}BB^T - \frac{1}{\rho^2}LL^T)P \tag{66}$$

Moreover, the following feedback control law is applied to the system

$$u = -\frac{1}{r}B^T Pe \tag{67}$$

By substituting Eq. (66) and Eq. (67) into Eq. (65) and by performing intermediate operations one obtains

$$\begin{gathered}\dot{V} = \frac{1}{2}e^T[-Q + P(\frac{2}{r}BB^T - \frac{1}{2\rho^2}LL^T)P]e + e^T PB(-\frac{1}{r}B^T Pe) + e^T PL\tilde{d} \Rightarrow \\ \dot{V} = -\frac{1}{2}e^T Qe + (\frac{1}{r}e^T PBB^T Pe - \frac{1}{2\rho^2}e^T PLL^T Pe) - \frac{1}{r}e^T PBB^T Pe) + e^T PL\tilde{d} \Rightarrow \\ \dot{V} = -\frac{1}{2}e^T Qe - \frac{1}{2\rho^2}e^T PLL^T Pe + e^T PL\tilde{d} \Rightarrow \\ \dot{V} = -\frac{1}{2}e^T Qe - \frac{1}{2\rho^2}e^T PLL^T Pe + \frac{1}{2}e^T PL\tilde{d} + \frac{1}{2}\tilde{d}^T L^T Pe\end{gathered} \tag{68}$$

Lemma: The following inequality holds

$$\tfrac{1}{2}e^T PL\tilde{d} + \tfrac{1}{2}\tilde{d}L^T Pe - \tfrac{1}{2\rho^2}e^T PLL^T Pe \leq \tfrac{1}{2}\rho^2 \tilde{d}^T\tilde{d} \tag{69}$$

Proof: The binomial $(\rho\alpha - \frac{1}{\rho}b)^2$ is considered. Expanding the left part of the above inequality one gets

$$\begin{array}{c} \rho^2 a^2 + \frac{1}{\rho^2}b^2 - 2ab \geq 0 \Rightarrow \frac{1}{2}\rho^2 a^2 + \frac{1}{2\rho^2}b^2 - ab \geq 0 \Rightarrow \\ ab - \frac{1}{2\rho^2}b^2 \leq \frac{1}{2}\rho^2 a^2 \Rightarrow \frac{1}{2}ab + \frac{1}{2}ab - \frac{1}{2\rho^2}b^2 \leq \frac{1}{2}\rho^2 a^2 \end{array} \tag{70}$$

The following substitutions are carried out: $a = \tilde{d}$ and $b = e^T PL$ and the previous relation becomes

$$\tfrac{1}{2}\tilde{d}^T L^T Pe + \tfrac{1}{2}e^T PL\tilde{d} - \tfrac{1}{2\rho^2}e^T PLL^T Pe \leq \tfrac{1}{2}\rho^2 \tilde{d}^T\tilde{d} \tag{71}$$

Eq. (71) is substituted in the last row of Eq. (68) and the inequality is enforced, thus giving

$$\dot{V} \leq -\tfrac{1}{2}e^T Qe + \tfrac{1}{2}\rho^2 \tilde{d}^T\tilde{d} \tag{72}$$

Eq. (72) shows that the H_∞ tracking performance criterion is satisfied. The integration of $\dot{V}$ from 0 to T gives

$$\begin{array}{c} \int_0^T \dot{V}(t)dt \leq -\frac{1}{2}\int_0^T ||e||_Q^2 dt + \frac{1}{2}\rho^2 \int_0^T ||\tilde{d}||^2 dt \Rightarrow \\ 2V(T) + \int_0^T ||e||_Q^2 dt \leq 2V(0) + \rho^2 \int_0^T ||\tilde{d}||^2 dt \end{array} \tag{73}$$

Moreover, if there exists a positive constant $M_d > 0$ such that $\int_0^\infty ||\tilde{d}||^2 dt \leq M_d$ then one gets

$$\int_0^\infty ||e||_Q^2 dt \leq 2V(0) + \rho^2 M_d \tag{74}$$

Thus, the integral $\int_0^\infty ||e||_Q^2 dt$ is bounded. Moreover, $V(T)$ is bounded and from the definition of the Lyapunov function V in Eq. (63) it becomes clear that $e(t)$ will be also bounded since $e(t) \in \Omega_e = \{e | e^T Pe \leq 2V(0) + \rho^2 M_d\}$. According to the above and with the use of Barbalat's Lemma one obtains $lim_{t\to\infty} e(t) = 0$.

After following the stages of the stability proof one arrives at Eq. (72) which shows that the H-infinity tracking performance criterion holds. By selecting the attenuation coefficient ρ to be sufficiently small and in particular to satisfy $\rho^2 < ||e||_Q^2 / ||\tilde{d}||^2$ one has that the first derivative of the Lyapunov function is upper bounded by 0. This condition holds at each sampling instance and consequently global stability for the control loop can be concluded.

4.2 Robust state estimation with Kalman Filtering

The control loop has to be implemented with the use of information provided by a small number of sensors and by processing only a small number of state variables. For instance, one can implement feedback control by measuring only state variables x_1, x_3, x_5, x_7, x_9, x_{11} that is the cartesian coordinates (x, y, z) of the autonomous tilt-rotor UAV and the rotation angles $\phi, \theta.\psi$ around the axes of the inertial reference system. To reconstruct the missing information about the state vector of the autonomous tilt-rotor UAV it is proposed to use a filtering scheme and based on it to apply state estimation-based control [1-3]. The recursion of the H_∞ Kalman Filter, for the tilt rotor UAV's model, can be formulated in terms of a *measurement update* and a *time update* part

Measurement update:

$$\begin{array}{l} D(k) = [I - \theta W(k)P^-(k) + C^T(k)R(k)^{-1}C(k)P^-(k)]^{-1} \\ K(k) = P^-(k)D(k)C^T(k)R(k)^{-1} \\ \hat{x}(k) = \hat{x}^-(k) + K(k)[y(k) - C\hat{x}^-(k)] \end{array} \tag{75}$$

Time update:

$$\begin{aligned} \hat{x}^{-}(k+1) &= A(k)x(k) + B(k)u(k) \\ P^{-}(k+1) &= A(k)P^{-}(k)D(k)A^{T}(k) + Q(k) \end{aligned} \tag{76}$$

where it is assumed that parameter θ is sufficiently small to assure that the covariance matrix $P^{-}(k)^{-1} - \theta W(k) + C^{T}(k)R(k)^{-1}C(k)$ will be positive definite. When $\theta = 0$ the H_{∞} Kalman Filter becomes equivalent to the standard Kalman Filter. One can measure only a part of the state vector of the autonomous tilt-rotor UAV, and can estimate through filtering the rest of the state vector elements [1],[4].

5 Simulation tests

The performance of the perviously analyzed nonlinear optimal control method for the dynamic model of the autonomous tilt-rotor UAV has been further confirmed through simulation tests. The numerical values of the model model of the tilted quadrotor where in accordance to [29-31]. To implement the nonlinear optimal control method the algebraic Riccati equation of Eq. (66) had to be repetitively solved at each time-step of the control algorithm, with the use of Matlab's function *aresolv()*. Besides, the Jacobian matrices of the system were also updated at each sampling instance. The obtained results are depicted in Fig. 3 to Fig. 22. The measurement units for the cartesian coordinates of the drone were in meters (m) and for its rotation angles were in radians (rad). The real values of the state variables of the tilt-rotor UAV are depicted in blue, their estimated values which have been provided by the H-infinity Kalman Filter are plotted in green while the associated reference setpoints are printed in red. The simulation results have shown that the nonlinear optimal control scheme achieves fast and accurate tracking of setpoints under moderate variations of the control inputs. Moreover, in Fig. 23 to Fig. 24 3D diagrams are given about the tracking of reference trajectories by the center-of-gravity of the tilt-rotor UAV.

The transient performance of the control method depends mainly of gains r, ρ and on gain matrix Q which appear in the Riccati equation of Eq. (66). Actually, by assigning small values to r one can achieve elimination of the state vector's tracking error, while by assigning relatively large values to the diagonal elements of matrix Q one can achieve fast convergence of state variables to setpoints. Moreover, the smallest value of ρ for which one can obtain a valid solution for the above-noted Riccati equation (in the form of positive-definite and symmetric matrix P) is the one that provides the control loop with maximum robustness. The nonlinear optimal control method results into minimization of energy dispersion by the actuators of the tilt-rotor UAV, thus increasing the autonomy and operational capacity of the drone. The method exhibits global (and not local) stability properties as it is confirmed by its ability to track time-varying and abruptly changing setpoints.

The nonlinear optimal control approach exhibits advantages against other control schemes one could have considered for the tilt-rotor UAV dynamics. For instance: (1) comparing to the global linearization-based control schemes (such as Lie algebra-based control or flatness-based control) it does not require complicated changes of state variables (diffeomorphisms) and transformation of the system's state-space description. Consequently, it also avoids inverse transformations which may come against singularity problems (2) comparing to Nonlinear Model Predictive Control, the proposed nonlinear optimal control method is of proven global stability and the convergence of its iterative search for an optimum does not depend on initialization and controller's parametrization, (3) comparing to sliding-mode control and backstepping control the application of the nonlinear optimal contorl method is not constrained into dynamical systems of a specific state-space form. It is known that unless the controlled system is found in the input-output linearized form the definition of the associated sliding surfaces is an empirical procedure. Besides, unless the controlled system is found in the backstepping integral (triangular) form, the application of backstepping control is not possible (4) comparing to PID control the nonlinear optimal control method is of proven global stability and its performance is not dependant on heuristics-based selection of parameters of the controller, (5)

comparing to multiple-models based optimal control, the nonlinear optimal control method requires the computation of only one linearization point and the solution of only one Riccati equation.

To elaborate on the tracking performance and on the robustness of the proposed nonlinear optimal control method for the tilt-rotor UAV the following Tables are given: (i) Table I which provides information about the accuracy of tracking of the reference setpoints by the state variables of the tilt rotor UAV's state-space model, (ii) Table II which provides information about the robustness of the control method to parametric changes in the model of the tilt rotor UAV's dynamics (change $\Delta a\%$ in the mass m of the drone), (iii) Table III which provides information about the precision in state variables' estimation that is achieved by the H-infinity Kalman Filter, (iv) Table IV which provides the approximate convergence time of the tilt rotor UAV's state variables to the associated setpoints.

Table I

Tracking RMSE for the tilt-rotor UAV in the disturbance-free case

	$RMSE_{x_1}$	$RMSE_{x_2}$	$RMSE_{x_3}$	$RMSE_{x_4}$	$RMSE_{x_5}$	$RMSE_{x_6}$	$RMSE_{x_7}$	$RMSE_{x_9}$	$RMSE_{x_{11}}$
test_1	0.0098	0.0001	0.0047	0.0001	0.0089	0.0001	0.0001	0.0001	0.0036
test_2	0.0074	0.0001	0.0033	0.0001	0.0069	0.0001	0.0001	0.0001	0.0031
test_3	0.0078	0.0001	0.0047	0.0001	0.0089	0.0001	0.0001	0.0001	0.0036
test_4	0.0095	0.0001	0.0040	0.0001	0.0066	0.0001	0.0001	0.0001	0.0041
test_5	0.0125	0.0001	0.0073	0.0001	0.0152	0.0002	0.0001	0.0002	0.0048
test_6	0.0103	0.0001	0.0045	0.0001	0.0090	0.0001	0.0001	0.0001	0.0045
test_7	0.0108	0.0002	0.0048	0.0001	0.0095	0.0001	0.0002	0.0001	0.0041
test_8	0.0098	0.0001	0.0030	0.0021	0.0067	0.0001	0.0001	0.0001	0.0042
test_9	0.0092	0.0001	0.0033	0.0008	0.0072	0.0008	0.0001	0.0001	0.0034
test_{10}	0.0103	0.005	0.0021	0.0005	0.0067	0.0006	0.0001	0.0001	0.0036

Table II

Tracking RMSE for the tilt-rotor UAV in the case of disturbances

$\Delta a\%$	$RMSE_{x_1}$	$RMSE_{x_2}$	$RMSE_{x_3}$	$RMSE_{x_4}$	$RMSE_{x_5}$	$RMSE_{x_6}$	$RMSE_{x_7}$	$RMSE_{x_9}$	$RMSE_{x_{11}}$
0%	0.0074	0.0001	0.0033	0.0001	0.0069	0.0001	0.0001	0.0001	0.0031
10%	0.0076	0.0001	0.0036	0.0001	0.0073	0.0001	0.0001	0.0001	0.0030
20%	0.0077	0.0001	0.0040	0.0001	0.0078	0.0001	0.0001	0.0001	0.0028
30%	0.0078	0.0001	0.0044	0.0001	0.0084	0.0001	0.0001	0.0001	0.0026
40%	0.0077	0.0001	0.0048	0.0001	0.0088	0.0001	0.0001	0.0001	0.0022
50%	0.0074	0.0061	0.0051	0.0001	0.0092	0.0001	0.0001	0.0001	0.0018
60%	0.0070	0.0001	0.0052	0.0001	0.0083	0.0001	0.0001	0.0001	0.0013

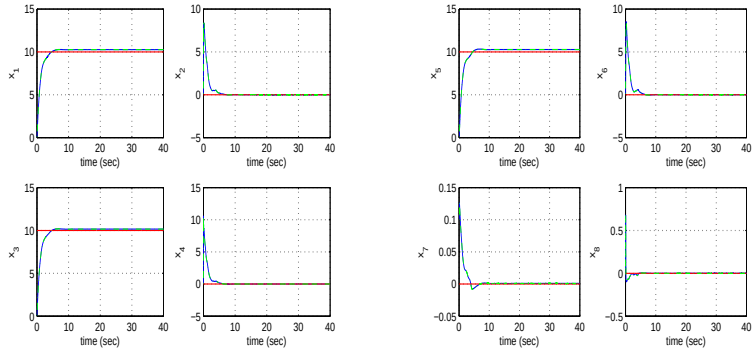

(a) **(b)**

Figure 3: Tracking of setpoint 1 for the tilt-rotor UAV, that is motion from initial position (x_A, y_A, z_A) to final position (x_B, y_B, z_B) and alignment of its rotation angles (a) convergence of state variables x_1 to x_4 to their reference setpoints (red line: setpoint, blue line: real value, green line: estimated value), (b) convergence of state variables x_5 to x_8 to their reference setpoints (red line: setpoint, blue line: real value, green line: estimated value)

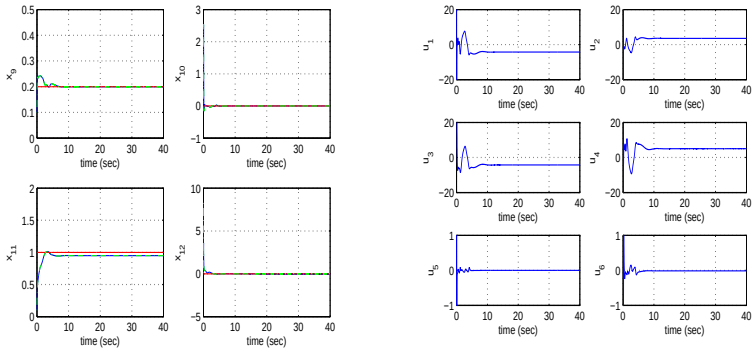

(a) **(b)**

Figure 4: Tracking of setpoint 1 for the tilt-rotor UAV, that is motion from initial position (x_A, y_A, z_A) to final position (x_B, y_B, z_B) and alignment of its rotation angles (a) convergence of state variables x_9 to x_{12} to their reference setpoints (red line: setpoint, blue line: real value, green line: estimated value), (b) real control inputs u_1 to u_6

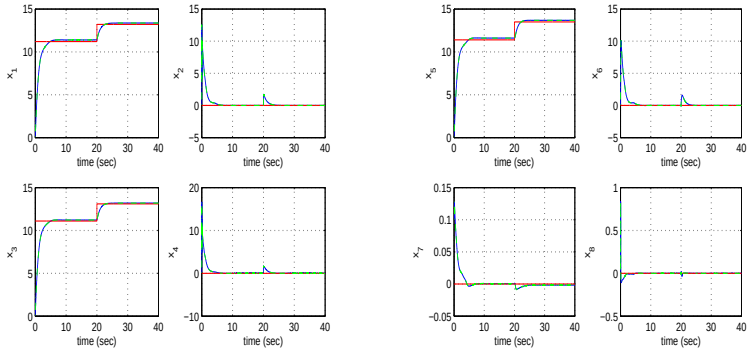

(a) **(b)**

Figure 5: Tracking of setpoint 2 for the tilt-rotor UAV, that is motion from initial position (x_A, y_A, z_A) to final position (x_B, y_B, z_B) and alignment of its rotation angles (a) convergence of state variables x_1 to x_4 to their reference setpoints (red line: setpoint, blue line: real value, green line: estimated value), (b) convergence of state variables x_5 to x_8 to their reference setpoints (red line: setpoint, blue line: real value, green line: estimated value)

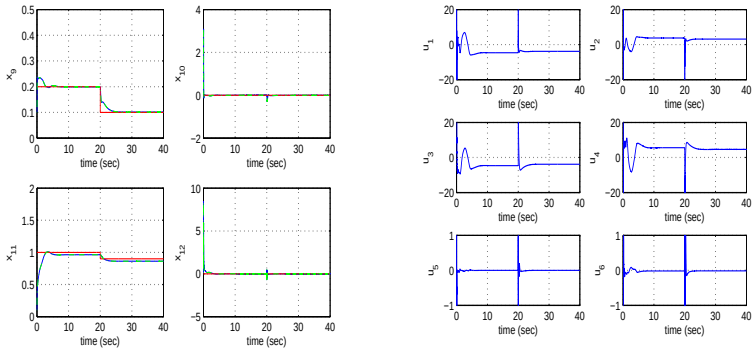

(a) **(b)**

Figure 6: Tracking of setpoint 2 for the tilt-rotor UAV, that is motion from initial position (x_A, y_A, z_A) to final position (x_B, y_B, z_B) and alignment of its rotation angles (a) convergence of state variables x_9 to x_{12} to their reference setpoints (red line: setpoint, blue line: real value, green line: estimated value), (b) real control inputs u_1 to u_6

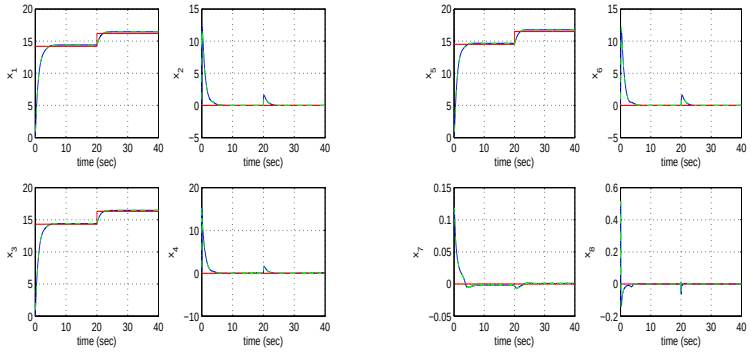

(a) **(b)**

Figure 7: Tracking of setpoint 3 for the tiltrotor UAV, that is motion from initial position (x_A, y_A, z_A) to final position (x_B, y_B, z_B) and alignment of its rotation angles (a) convergence of state variables x_1 to x_4 to their reference setpoints (red line: setpoint, blue line: real value, green line: estimated value), (b) convergence of state variables x_5 to x_8 to their reference setpoints (red line: setpoint, blue line: real value, green line: estimated value)

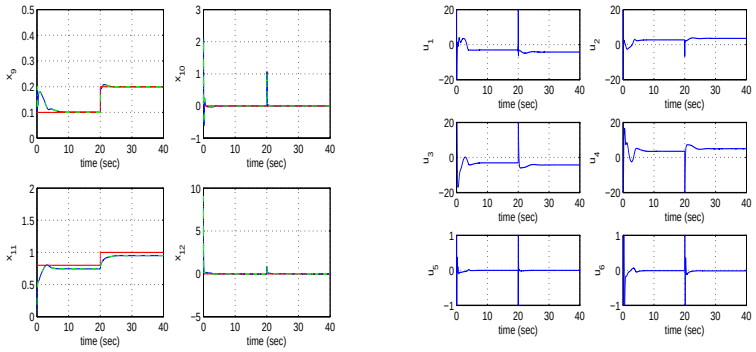

(a) **(b)**

Figure 8: Tracking of setpoint 3 for the tilt-rotor UAV, that is motion from initial position (x_A, y_A, z_A) to final position (x_B, y_B, z_B) and alignment of its rotation angles (a) convergence of state variables x_9 to x_{12} to their reference setpoints (red line: setpoint, blue line: real value, green line: estimated value), (b) real control inputs u_1 to u_6

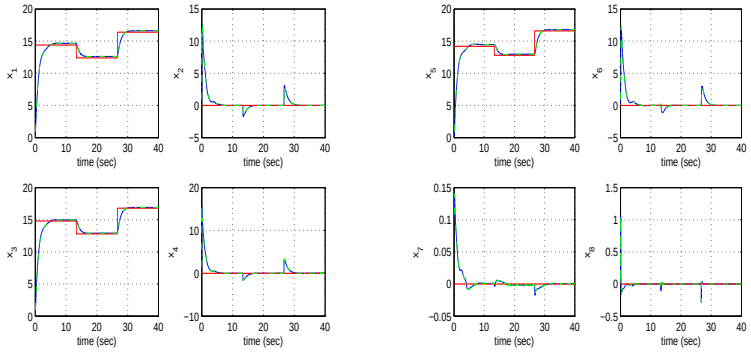

(a) **(b)**

Figure 9: Tracking of setpoint 4 for the tilt-rotor UAV, that is motion from initial position (x_A, y_A, z_A) to final position (x_B, y_B, z_B) and alignment of its rotation angles (a) convergence of state variables x_1 to x_4 to their reference setpoints (red line: setpoint, blue line: real value, green line: estimated value), (b) convergence of state variables x_5 to x_8 to their reference setpoints (red line: setpoint, blue line: real value, green line: estimated value)

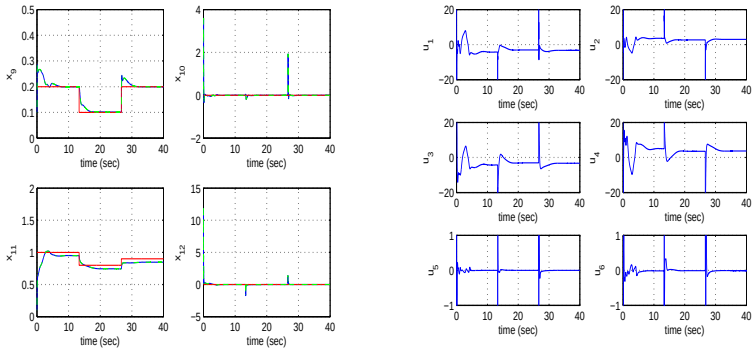

(a) **(b)**

Figure 10: Tracking of setpoint 4 for the tilt-rotor UAV, that is motion from initial position (x_A, y_A, z_A) to final position (x_B, y_B, z_B) and alignment of its rotation angles (a) convergence of state variables x_9 to x_{12} to their reference setpoints (red line: setpoint, blue line: real value, green line: estimated value), (b) real control inputs u_1 to u_6

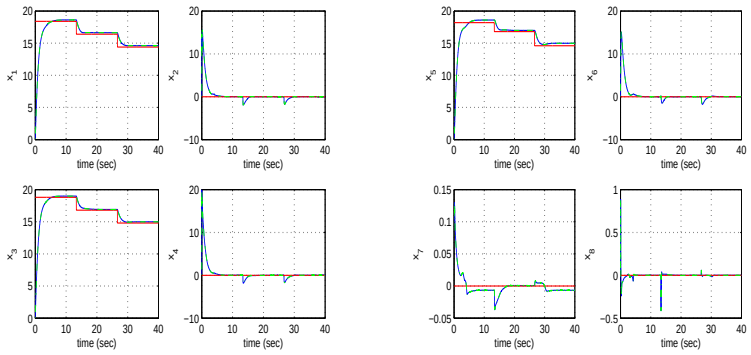

(a) **(b)**

Figure 11: Tracking of setpoint 5 for the tilt-rotor UAV, that is motion from initial position (x_A, y_A, z_A) to final position (x_B, y_B, z_B) and alignment of its rotation angles (a) convergence of state variables x_1 to x_4 to their reference setpoints (red line: setpoint, blue line: real value, green line: estimated value), (b) convergence of state variables x_5 to x_8 to their reference setpoints (red line: setpoint, blue line: real value, green line: estimated value)

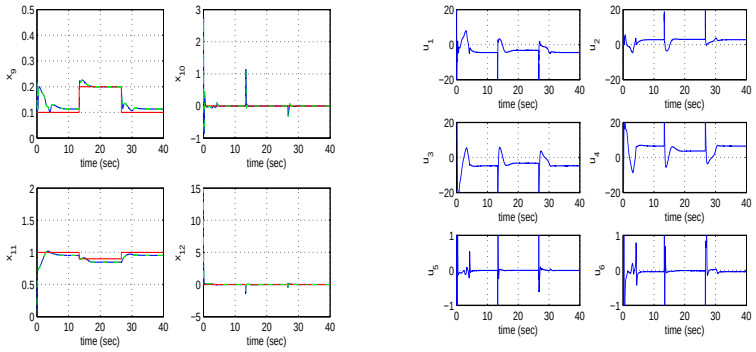

(a) **(b)**

Figure 12: Tracking of setpoint 5 for the tilt-rotor UAV, that is motion from initial position (x_A, y_A, z_A) to final position (x_B, y_B, z_B) and alignment of its rotation angles (a) convergence of state variables x_9 to x_{12} to their reference setpoints (red line: setpoint, blue line: real value, green line: estimated value), (b) real control inputs u_1 to u_6

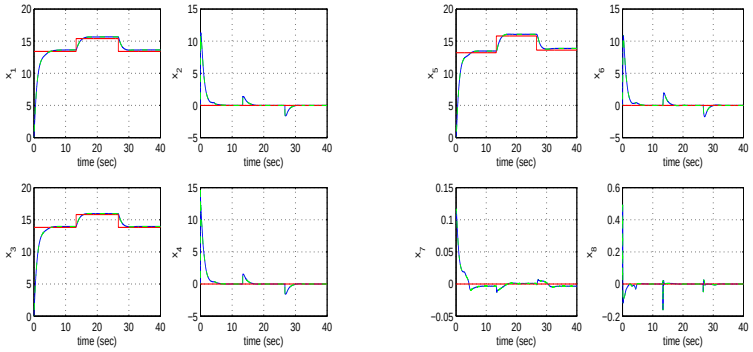

(a) **(b)**

Figure 13: Tracking of setpoint 6 for the tilt-rotor UAV, that is motion from initial position (x_A, y_A, z_A) to final position (x_B, y_B, z_B) and alignment of its rotation angles (a) convergence of state variables x_1 to x_4 to their reference setpoints (red line: setpoint, blue line: real value, green line: estimated value), (b) convergence of state variables x_5 to x_8 to their reference setpoints (red line: setpoint, blue line: real value, green line: estimated value)

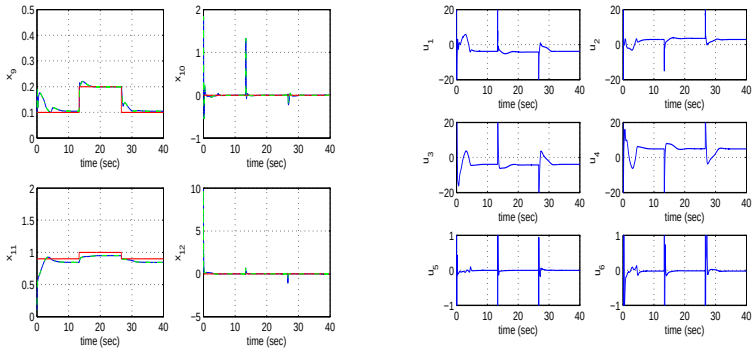

(a) **(b)**

Figure 14: Tracking of setpoint 6 for the tilt-rotor UAV, that is motion from initial position (x_A, y_A, z_A) to final position (x_B, y_B, z_B) and alignment of its rotation angles (a) convergence of state variables x_9 to x_{12} to their reference setpoints (red line: setpoint, blue line: real value, green line: estimated value), (b) real control inputs u_1 to u_6

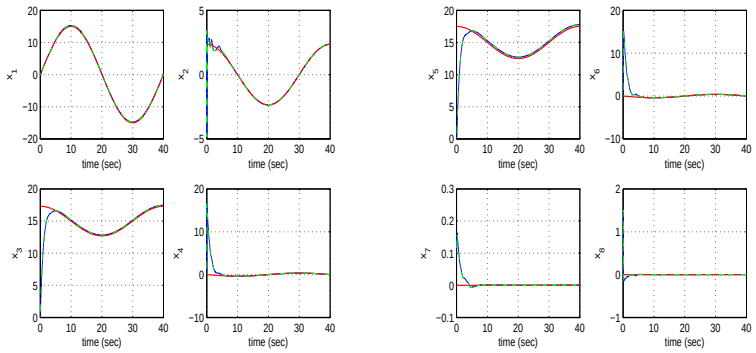

(a) **(b)**

Figure 15: Tracking of setpoint 7 for the tilt-rotor UAV, that is motion along a sinusoidal trajectory and alignment of its rotation angles (a) convergence of state variables x_1 to x_4 to their reference setpoints (red line: setpoint, blue line: real value, green line: estimated value), (b) convergence of state variables x_5 to x_8 to their reference setpoints (red line: setpoint, blue line: real value, green line: estimated value)

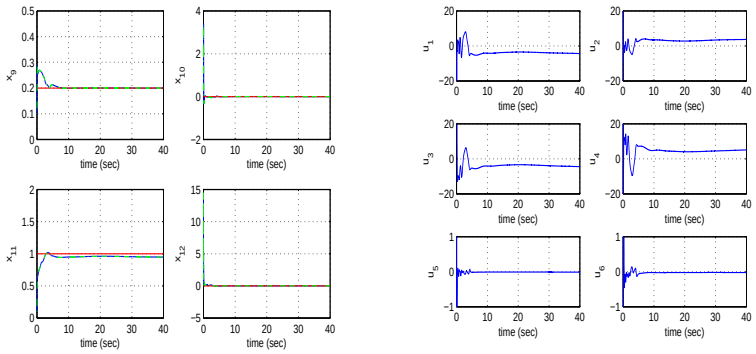

(a) **(b)**

Figure 16: Tracking of setpoint 7 for the tilt-rotor UAV, that is motion along a sinusoidal trajectory and alignment of its rotation angles (a) convergence of state variables x_9 to x_{12} to their reference setpoints (red line: setpoint, blue line: real value, green line: estimated value), (b) real control inputs u_1 to u_6

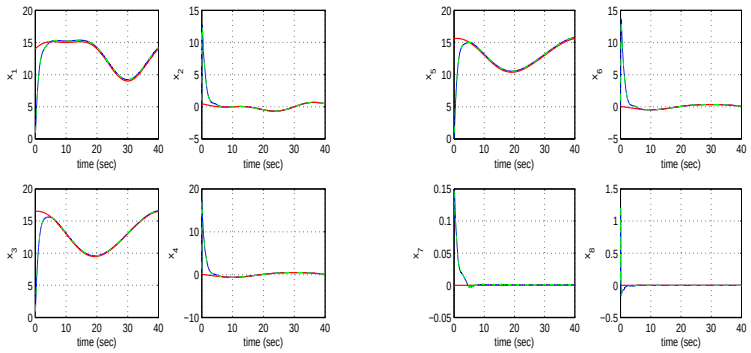

(a) **(b)**

Figure 17: Tracking of setpoint 8 for the tilt-rotor UAV, that is motion along a sinusoidal trajectory and alignment of its rotation angles (a) convergence of state variables x_1 to x_4 to their reference setpoints (red line: setpoint, blue line: real value, green line: estimated value), (b) convergence of state variables x_5 to x_8 to their reference setpoints (red line: setpoint, blue line: real value, green line: estimated value)

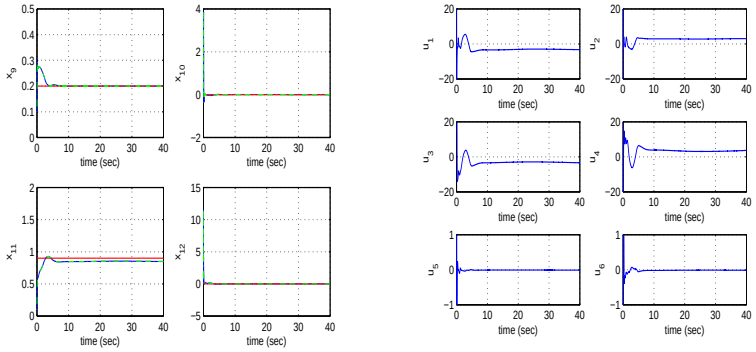

(a) **(b)**

Figure 18: Tracking of setpoint 8 for the tilt-rotor UAV, that is motion along a sinusoidal trajectory and alignment of its rotation angles (a) convergence of state variables x_9 to x_{12} to their reference setpoints (red line: setpoint, blue line: real value, green line: estimated value), (b) real control inputs u_1 to u_6

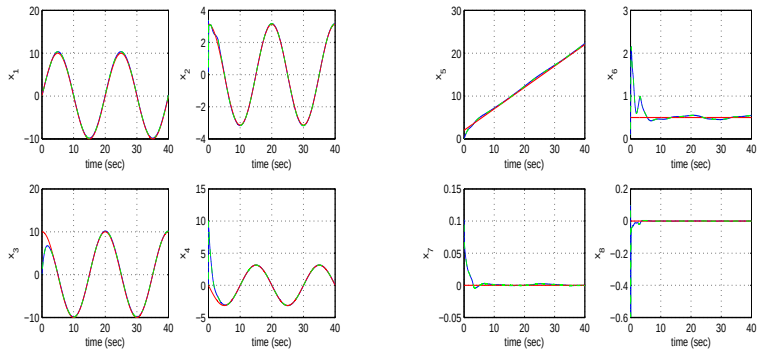

(a) **(b)**

Figure 19: Tracking of setpoint 9 for the tilt-rotor UAV, that is motion along a sinusoidal trajectory and alignment of its rotation angles (a) convergence of state variables x_1 to x_4 to their reference setpoints (red line: setpoint, blue line: real value, green line: estimated value), (b) convergence of state variables x_5 to x_8 to their reference setpoints (red line: setpoint, blue line: real value, green line: estimated value)

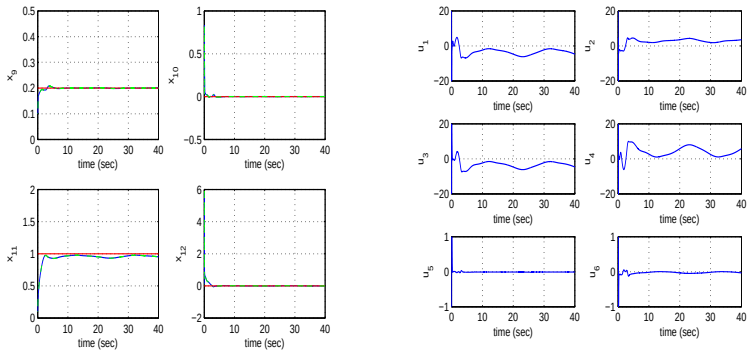

(a) **(b)**

Figure 20: Tracking of setpoint 9 for the tilt-rotor UAV, that is motion along a sinusoidal trajectory and alignment of its rotation angles (a) convergence of state variables x_9 to x_{12} to their reference setpoints (red line: setpoint, blue line: real value, green line: estimated value), (b) real control inputs u_1 to u_6

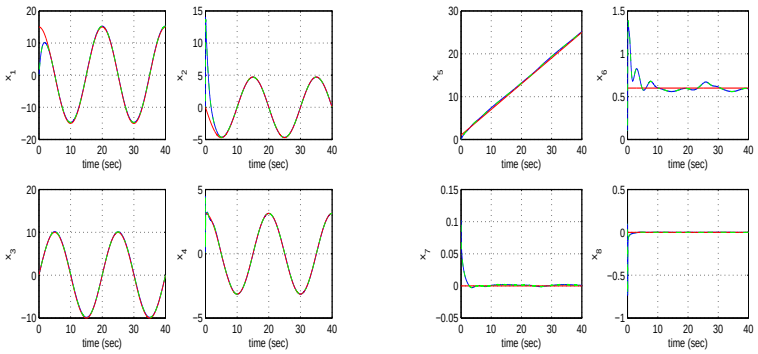

(a) (b)

Figure 21: Tracking of setpoint 10 for the tilt-rotor UAV, that is motion along a sinusoidal trajectory and alignment of its rotation angles (a) convergence of state variables x_1 to x_4 to their reference setpoints (red line: setpoint, blue line: real value, green line: estimated value), (b) convergence of state variables x_5 to x_8 to their reference setpoints (red line: setpoint, blue line: real value, green line: estimated value)

Table III

RMSE $\times 10^{-4}$ for the estimation performed by the H-infinity KF

	$RMSE_{x_1}$	$RMSE_{x_2}$	$RMSE_{x_3}$	$RMSE_{x_4}$	$RMSE_{x_5}$	$RMSE_{x_6}$	$RMSE_{x_7}$	$RMSE_{x_9}$	$RMSE_{x_{11}}$
test_1	0.0910	0.1559	0.1039	0.0943	0.0959	0.1046	0.1099	0.1038	0.1110
test_2	0.1200	0.1034	0.1004	0.0877	0.1229	0.0918	0.1329	0.1202	0.0800
test_3	0.1009	0.1001	0.1255	0.0980	0.0905	0.1501	0.1057	0.0881	0.1001
test_4	0.1108	0.0966	0.0899	0.0876	0.1038	0.1092	0.1299	0.0844	0.1097
test_5	0.1037	0.1153	0.1053	0.0980	0.1015	0.1094	0.0912	0.1116	0.0893
test_6	0.0980	0.1180	0.1047	0.0917	0.1112	0.0897	0.1086	0.1092	0.1030
test_7	0.1076	0.1006	0.0954	0.1011	0.1098	0.1187	0.1000	0.1024	0.1247
test_8	0.1342	0.1040	0.0984	0.1088	0.1021	0.0972	0.0938	0.1260	0.1184
test_9	0.1229	0.1128	0.0867	0.0849	0.1250	0.1210	0.0925	0.1073	0.1015
test_{10}	0.1140	0.1156	0.0958	0.0928	0.1124	0.1070	0.0988	0.0877	0.1010

Table IV

Convergence time (sec) for the tilt-rotor UAV state variables

	T_s x_1	T_s x_2	T_s x_3	T_s x_4	T_s x_5	T_s x_6	T_s x_7	T_s x_9	T_s x_{11}
test_1	5	7	5	5	4	5	5	7	5
test_2	4	5	4	5	4	5	5	3	6
test_3	4	4	4	4	5	5	5	4	6
test_4	4	5	4	5	5	5	4	4	5
test_5	5	5	5	4	5	4	5	8	7
test_6	5	5	4	5	5	4	7	7	8
test_7	1	4	4	4	4	3	4	6	6
test_8	4	6	5	4	5	4	5	3	6
test_9	1	1	4	5	1	5	5	2	7
test_{10}	4	5	1	1	1	7	4	1	3

The proposed nonlinear optimal control method for tilt-rotor UAVs exhibits global (and not local) stability properties. This is explicitly proven through the article's Lyapunov stability analysis and experimentally

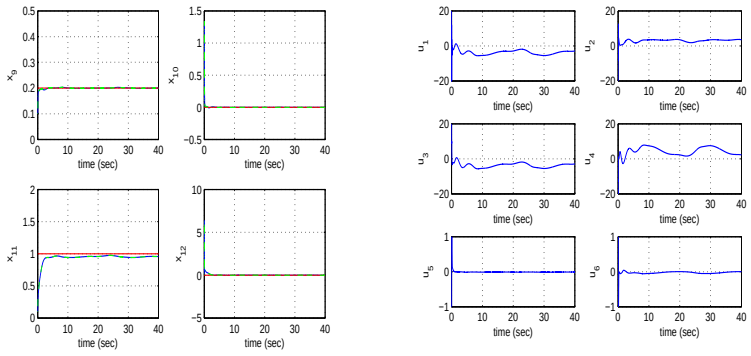

(a) (b)

Figure 22: Tracking of setpoint 10 for the tilt-rotor UAV, that is motion along a sinusoidal trajectory and alignment of its rotation angles (a) convergence of state variables x_9 to x_{12} to their reference setpoints (red line: setpoint, blue line: real value, green line: estimated value), (b) real control inputs u_1 to u_6

confirmed through the article's Simulation tests. The article's Lyapunov stability proof makes use of the tracking error dynamics of the initial nonlinear system. The computed control inputs are applied to the initial nonlinear model of the UAV and not to its linear approximation. It is ensured that the linearization error due to truncation of higher-order terms in the Taylor-series expansion remains small because the linearization process is performed at each sampling period around the present value of the UAV's state vector and not at a point on the desirable trajectory. By taking the span between the linearization point and the system's state vector at each sampling period to be small one concludes that the model which is obtained from linearization describes with precision the initial nonlinear dynamics of the UAV.

6 Conclusions

Due to nonlinearities and the multi-variable structure of the dynamic model of tilt-rotor UAVs the associated nonlinear control problem is a non-trivial one. The article has presented one of the few existing methods for treating the nonlinear optimal control problem of tilt-rotor UAVs. The dynamic model of tilt-rotor UAVs has been formulated in matrix form and its differential flatness properties have been analyzed. Next, to implement the nonlinear optimal control method, the UAV's state-space model has undergone an approximate linearization procedure with the use of first-order Taylor series expansion and through the computation of the associated Jacobian matrices. The linearization process has been performed around a temporary operating point which was updated at each sampling instance and which was defined by the present value of the system's state vector and by the last sampled value of the control inputs vector. For the approximately linearized model of the drone a robust H-infinity controller was designed.

The proposed nonlinear optimal (H-infinity) controller represents a min-max differential game between two competing entities (i) the control inputs of the drone which try to minimize a quadratic cost function of the state vector's tracking error, (ii) the model uncertainty and exogenous perturbations which try to maximize this cost function. To select the stabilizing feedback gains of the optimal (H-infinity) controller an algebraic Riccati equation had to be repetitively solved at each time-step of the control method. The global stability properties of the control scheme have been proven through Lyapunov analysis. First, it has been demonstrated that the control method satisfies the H-infinity tracking performance criterion which signifies elevated robustness against model uncertainty and exogenous perturbations. Moreover, under

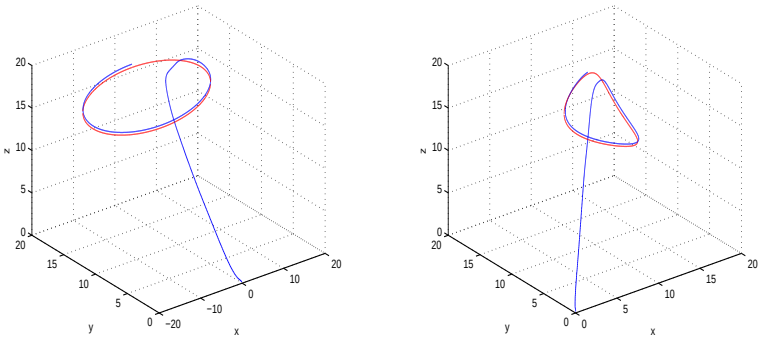

(a) (b)

Figure 23: Tracking of reference path in the cartesian space by the tilt-rotor UAV (red line: reference trajectory, blue line: path of the tilt-rotor UAV), (a) when tracking setpoint 7 (b) when tracking setpoint 8

moderate conditions it has been proven that the control loop becomes globally asymptotically stable. To perform state estimation-based control without the need to measure the entire state vetor of the tilt-rotor UAV, the H-infinity Kalman Filter has been used as a robust state estimator. The provided theoretical analysis and the method's experimental testing has confirmed that the nonlinear optimal control approach achieves fast and accurate tracking of reference setpoints under moderate variations of the control inputs.

References

[1] G. Rigatos and K. Busawon, Robotic manipulators and vehicles: Control, estimation and filtering, Springer, 2018.

[2] G. Rigatos, Nonlinear control and filtering using differential flatness theory: applications to electromechanical systems, Springer, 2015.

[3] G. Rigatos and E. Karapanou, Advances in applied nonlinear optimal control, Cambridge Scholars Publishing, 2020.

[4] G. Rigatos, M. Abbaszadeh and P. Siano, Control and estimation of dynamical nonlinear and partial differential equation systems: Theory and applications, IET Publications, 2022.

[5] G. Rigatos, Nonlinear Kalman Filters and Particle Filters for integrated navigation of unmanned aerial vehicles, Robotics and Autonomous Systems. Elsevier, vol. 60. no. 7, pp. 978-995, 2012.

[6] W. Hua, B. Xian and T. Xia, Fault tolerant position tracking control design for a tilt tri-rotor unmanned aerial vehicle, IEEE Transactions on Industrial Electonics, vol. 69, no. 1, pp. 604-612, 2022.

[7] Z. Liu, D. Theilliol, L. Yang, Y. He and J. Hou, Observer-based linear parameter varying control design with unmeasurable varying parameters under sensor fault for a quad-tile rotor unmanned aerial vehicle, Aerospace Science and Technology, Elsevier, vol. 92, pp. 696-719, 2019.

[8] Y. Su, L. Ruan, P, Yu, C.H. Pi, M.J. Gerber and T.C. Tsao, A fast and efficient attitude control algorithm of a tilt-rotor aerial platform using input redundanctes, IEEE Robotics and Automation Letters, vol. 7, no. 2, pp. 1214-1221, 2022.

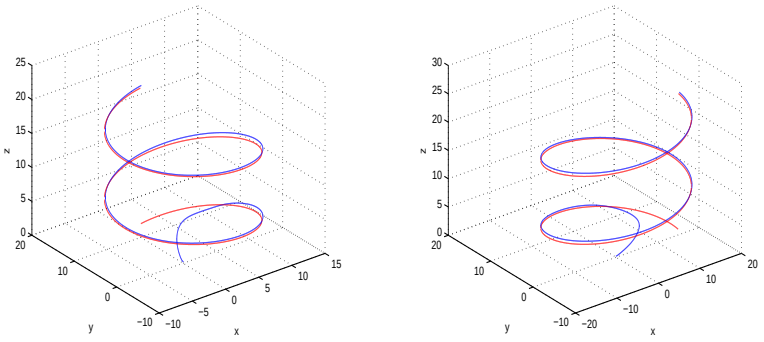

(a) (b)

Figure 24: Tracking of reference path in the cartesian space by the tilt-rotor UAV (red line: reference trajectory, blue line: path of the tilt-rotor UAV), (a) when tracking setpoint 9 (b) when tracking setpoint 10

[9] O. Invernissi, M. Giurato, P. Guitazzo and M. Lovera, Comparison of control methods for trajectory tracking in fully automated unmanned aerial vehicle, IEEE Transactions on Control Systems Technology, vol. 29, no. 3, pp. 1143-1164, 2021

[10] L. Yu, G. He, S. Zhao, X. Wang and L. Shen, Immersion and invariance-based sliding-mode attitude control of tilt tri-rotor UAV in helicopter mode, Intl. Journal of Control, Automation and Systems, Springer, vol. 16, no. 4, pp. 1-14, 2021.

[11] W. Zhou, X. Wang, X. Wang, W. Wang and B. Liu, Design of sliding-mode controller for tilting quadrotor UAV based on predetermined performance, Journal of Physics Conference Series, vol. 1748, no. 062074, pp. 1-9, 2021

[12] N. Thirumaleshwar Hedge, V.I. George, C. Gurada Nayak and A. Clayeus Vaz, Applications of robust H-infinity controller in transition flight modelling of autonomous VTOL convertible quad-tilt rotor UAV, Intl. Journal of Intelligent Unmanned Systems, Emerald Publishing, vol. 9, no. 3, pp. 204-235, 2021.

[13] N. Thirumaleshwar Hedge, V.I. George, and C. Gurada Nayak, Design dynamics modellign and control of tilt-rotor UAVs: a review, Intl. Journal of Intelligent Unmanned Systems, Emerald Publishing, vol. 8, no. 3, pp. 143-161, 2020.

[14] Q. Zhang, J. Zhang, X. Wang, Y. Xu and Z. Yu, Wind field disturbance analysis and flight control system design for a novel tilt-rotor UAV, IEEE Access, vol. 8, pp. 211401-211410, 2020

[15] B. Xian and W. Hao, Nonlinear robust fault tolerant control fo the tilt-rotor UAV under rear servo's stuck fault: Theory and experiments, IEEE Transactions on Industrial Informatics, vol. 15, no. 4, pp. 2158-2166, 2019.

[16] B.S. Reyo and G.V. Raffo, Suspended load path tracking control using a tilt-rotor UAV based on zonotopic state estimation, Journal of the Franklin Institute, Elsevier, vol. 356, pp. 1695-1729, 2019.

[17] A. Prach and E. Kayacan, An MPC-based position controller for a tilt-rotor tricopter VTOL UAV, Optimal Control Applications and Methods, J. Wiley, vol. 39, no. 1, pp. 343-356, 2018

[18] S. Park, J. Bue, Y. Kim and S. Kim, Fault tolerant flight control system for the tilt-rotor UAV, Journal of the Franklin Institute, Elsevier, vol. 350, pp. 2535-2559, 2013.

[19] J.A. Ricardo Jr. and D.A. Santos, Smooth second-order sliding-mode control for fully-actuated multi-rotor aerial vehicle, ISA Transactions, Elsevier, 2022.

[20] P. Zheng, X. Tan, B. Bahadir Kocer, E. Yang and M. Kovac, Tilt Drone: A fully actuated tilting quadrotor platform, IEEE Robotics and Automation Letters, vol. 5, no. 4, pp. 6845-6852, 2020.

[21] W. Su, S. Qu, G. Zhu, S.S-Min Swei, M. Hashimoto, and T. Zeng, Modeling and control of a class of urban air mobility tilt-rotor aircraft, Journal of Aerospace Science and Technology, Elsevier, vol. 124, pp. 107561, 2022

[22] Y. Tadakoro, T, Ibaki and M. Sampei, Joint optimization of geometric control and structure of a fully-actuated Hexrotor based on analytic HJBE solution, IEEE CDC 2018, IEEE 2018 Conference on Decision and Control, Miami, Florida, Dec. 2018

[23] Y. Tadakoro, T. Ibaki and H. Sampoi, Nonlinear model-predictive control of a fully-actuated UAV on SE(3) using acceleration characteristics of the stricture, IEEE ASCC 2019, IEEE 2019 Asian Control Conference, KitaKyushu, Japan, June 2019.

[24] C. Ding and L. Lu, Modelling and control of fully actuated vector thrust unmanned aerial vehicles, Proc. IFSA 2018, The 2018 Intl. symposium on Flexible Automation, Kanazawa, Japan, July 2018.

[25] M. Ryll, H.H. Bulthoff and P. Robuffo Giordano, A novel overactuated quadrotor unmanned aerial vehicle: Modelling, control and experimental validation, IEEE Trandactions on Control Systems Technology, vol. 23, no. 2, pp. 540-556, 2015.

[26] R. Ji, J. Mi, S.S. Ge and R. Ji, Adaptive second-order sliding-mode control for a tilting quad-copter with input saturations, IFAC WC 2020, Proc. 21dt IFAC World Congress, Berlin, Germany, July 2020.

[27] M. Liu, R. Ji and S.S. Ge, Adaptive neural control for a tilting quadcopter wjth finite-time convergence, Neural Computing and Applications, Springer, vol. 33, pp. 15981-16004, 2021

[28] Y. Xu , X. Wang and J. Zhang, Real-time parameter identification method for a novel blended-wing-body tilt-rotor UAV, Measurement, Elsevier, vol. 196, pp. 111220, 2022

[29] S. Sridhar, G. Gupta, R. Kumar, M. Kumr and K. Cohen, Tilt-rotor quadropter explored: Hardware-based dynamics, smart sliding-mode controller, attitude hold and wind disturbance scenarios, IEEE ACC 2019, IEEE 2019 American Control Conference, Philadelphia, USA, July 2019

[30] A. Nemati and M. Kumar, Modelling and control of single-axis tilting quadropter, IEEE ACC 2014, IEEE 2014 American Control Conference, Portland, Oregon, USA, June 20144.

[31] A. Nemati and M. Kumar, Nonlinear control of tilting quad-copter using feedback linearization-based motion control, Proc. ASME Dynamic Systems and Contorl Division, DSCC 2014, San Antonio, Texas, USA, Oct. 2014.

[32] R. Kumar, A Nemati, M. Kumar, R. Sharma, K,. cohen and F. Cazaurang, Tilting motor quadcopter for aggresive flight maneuvers using differential flatness-based flight controller, Proc. ASME Dynamic Systems and Control Conference, DSCC 2017, Tysons, Virginia, USA, Oct. 2017

[33] S. Sridhar, R. Kumar, K. Cohen and M. Kumar, Fault-tolerance of a reconfigurable tilt-rotor quad-copter using sliding-mode control, Proc. ASME 2018, Dynamic Systems and Control Conference, Atlanta, Georgia, USA, Oct. 2019

[34] A. Nemati, R. Kumar and M. Kumar, Stabilzing and control of tilting-rotor quadropter in case of a propeller failure, Proc. AMSE Dynamic Systems and Control Division, DSCC 2016, Minnesota, USA, Oct. 2016.

[35] R. Kumar, S. Sridhar, F. Cazaurang, K. cohen and M. Kumar, Reconfigurable fault-tolerant tilt-rotor quadcopter system, Proc. ASME 2018 Dynamic Systems and Control Conference, DSCC 2018, Atlanta, Georgia, USA, Sep. 2018

[36] A. Nemati and M. Kumar, Nonlinear control of tilting quadropter using feedback linearization-based motion control, Proc. ASME Dynamic Systems and Control Division, DSCC 2014, San Antonio, USA, Oct. 2014

[37] G.G. Rigatos and S.G. Tzafestas, Extended Kalman Filtering for Fuzzy Modelling and Multi-Sensor Fusion, Mathematical and Computer Modelling of Dynamical Systems, Taylor & Francis (2007), 13, pp. 251-266.

[38] M. Basseville and I. Nikiforov, Detection of abrupt changes: Theory and Applications, *Prentice-Hall*, 1993.

[39] G. Rigatos and Q. Zhang, Fuzzy model validation using the local statistical approach, Fuzzy Sets and Systems, Elsevier, vol. 60, no. 7, pp. 882-904,2009.

[40] G. Rigatos, A Nonlinear Optimal Control Approach for the Vertical Take-off and Landing Aircraft, Journal of Guidance, Navigation and Control, World Scientific, vol. 1, po. 3, pp. 2150012, 2021

[41] G. Rigatos, A nonlinear optimal control approach for the UAV and suspended payload system, Journal of Cybernetics and Physics, vol. 10, no. 1, pp. 27-39, 2021

[42] G.J. Toussaint, T. Basar and F. Bullo, H_∞ optimal tracking control techniques for nonlinear under-actuated systems, in Proc. IEEE CDC 2000, 39th IEEE Conference on Decision and Control, Sydney Australia, 2000.